Processing LADCP/CTD Data For Vertical Velocity, Finescale Vertical Kinetic Energy Density and Turbulence Estimates (`LADCP_w` Software V1.4)

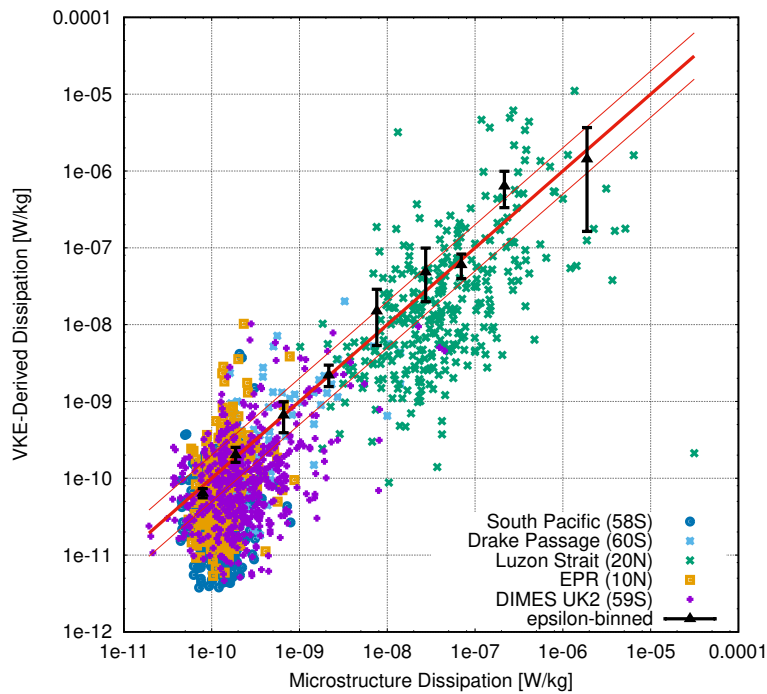A.M. Thurnherr

November 27, 2018

Figure 1: Parameterized kinetic energy dissipation from LADCP/CTD data processed with version 1.3 of the software described in this manual vs. dissipation from simultaneous microstructure profiles. Colored symbols: 320 m-averaged samples from 5 different data sets spanning a wide range of latitudes, turbulence levels, and dynamic regimes; in addition to 996 samples from the original data sets used to derive the parameterization *(Thurnherr et al.,* 2015), there are an additional 499 samples from the DIMES UK2 data set collected primarily in the region around Drake Passage; the new data set is fully consistent with the others. Error bars: $\epsilon_{\mu\text{structure}}$-bin-averaged ϵ_{VKE} with 95% confidence limits from bootstrapping, bins with fewer than 10 samples are not shown. Red lines: Equality within factor two.

1

Contents

1 Introduction

1.1 Preliminary Comments

This manual is intended as a "cookbook," describing how to derive profiles of vertical ocean velocity (w_{ocean}, Sections 2–4), Vertical Kinetic Energy (VKE) and VKE-derived dissipation (ϵ_{VKE}, Section 5) from data collected with standard LADCP/CTD systems, using processing software available at `http://www.ldeo.columbia.edu/LADCP`. *No special instrument setup is required for acquiring LADCP data suitable for vertical-velocity processing. In particular, vertical velocities can be calculated from archived LADCP data, as long as pressure time series of adequate temporal resolution and quality are available.* The software is a fairly complex implementation of a simple method that consists in subtracting vertical package velocity (w_{CTD}), derived from CTD pressure time series, from the ADCP-derived vertical velocity measurements (w_{ADCP}), before binning the resulting ocean velocities ($w_{\text{ocean}} = w_{\text{ADCP}} - w_{\text{CTD}}$) in depth *(Thurnherr, 2011)*. The processing software is implemented in the `perl` programming language and has been tested on UN*X systems, including MacOSX, FreeBSD and Linux. All source files use tab stops every 4 columns; for correct formatting use, e.g. `less -x4` or an editor where the tab separation can be changed.

Processing LADCP data for vertical ocean velocity is conceptually much simpler than horizontal-velocity processing *(Firing and Gordon, 1990; Fischer and Visbeck, 1993a; Visbeck, 2002)*. While the unknown horizontal CTD-package velocity required to obtain ocean velocity from the relative measurements must be inferred from external constraints in case of horizontal velocity, the vertical package velocity w_{CTD} is known at all times. This has several important consequences:

1. The vertical velocities at a given depth derived from the downlooker and from the uplooker are entirely independent, as they do not use any common data. (The two instrument sample the same depth at different times.) Differences between uplooker and downlooker-derived w_{ocean} data therefore provide a quantitative metric of measurement uncertainty.

2. Profiles with gaps, e.g. due to insufficient acoustic scattering at depth, can be processed without any particular difficulties.

3. Because of the random-walk error accumulation, instrument range is the most important parameter affecting the quality of horizontal LADCP velocities *(Firing and Gordon, 1990; Visbeck, 2002; Thurnherr, 2010)*. For vertical velocities, random error (but not bias) can be reduced by decreasing the vertical resolution of the binned profiles during post-processing. This allows calculation of w_{ocean} in some regions where the acoustic backscatter is too weak (instrument range too short) for horizontal-velocity processing.

There are additional important differences between processing LADCP data for horizontal and vertical velocities:

1. Horizontal ocean velocities are mostly dominated by processes with timescales that are long compared to typical LADCP/CTD cast durations. As a result, down- and upcast data are usually combined to yield cast-time averaged profiles. In contrast, vertical velocities are mostly dominated by internal waves near the buoyancy frequency (e.g. *Thurnherr et al.*, 2014), i.e. with time scales that are not long compared to typical CTD/LADCP sampling time scales. As a result, down- and upcast w_{ocean} data must be processed separately, yielding two profiles from each cast.

2. Good heading (compass) data are required for horizontal-velocity LADCP processing. LADCP data collected near the magnetic poles, in particular, cannot be processed for horizontal velocity. In contrast, heading data are not used at all for w_{ocean} LADCP processing, i.e. data from the magnetic poles or from instruments with bad compasses can be processed for vertical velocity.

There are different versions of the `LADCP_w` software. Each output file contains the version of the processing-software used to produce it in its header (meta-data). The diagnostic plots are also labeled with the processing version. Note that many of the plots in this guide have been produced with older versions of the software.

1.2   Software Requirements and Installation

The processing software for vertical LADCP velocities is implemented in the `perl` programming language, which is pre-installed on must UN*X systems. Diagnostic plots are produced with the `Generic Mapping Tools` (GMT), a set of UN*X tools to produce Postscript plots from ASCII input files. The following software is required to process LADCP/CTD data for vertical velocity:

Generic Mapping Tools (GMT) GMT must be installed and the GMT binary directory must be included in the search path of the shell.[1] GMT version 5 is required.

ANTSlib This library, available at `www.ldeo.columbia.edu/LADCP`, provides a general data processing and I/O framework. The installation directory must be added to the shell's search path.

ADCP_tools This tool kit provides additional required libraries, as well as a number of ADCP utilities, e.g. for splitting ADCP files from tow-yos and yo-yos into individual casts. The ADCP Tools are available at `www.ldeo.columbia.edu/LADCP`. The installation directory must be added to the shell's search path.

LADCP_w The vertical-velocity processing software is implemented as several separate command-line utilities. It is available at `www.ldeo.columbia.edu/LADCP`. The installation directory must be added to the shell's search path.

Once all required software has been installed, the installation can be tested by running

```
LADCP_w_ocean -V
```

from any directory. If any of the prerequisites are missing (or if the path is not set correctly) an error message is produced. If the installation is complete, a short version and copyright message is produced instead. Running `LADCP_w_ocean` or any other of the utilities described below without command-line arguments produces a usage message describing the command-line options and -arguments.

---

[1]Familiarity with basic UN*X shell concepts is assumed in this manual.

1.3 Vertical-Velocity Processing Overview

Vertical-velocity processing is carried out in several consecutive steps, which are implemented as separate command-line utilities to allow selective re-processing:

1. *Calculate vertical package velocity w_{CTD} with the LADCP_w_CTD utility.* Input: 24 Hz CTD time series. Output: 6 Hz time series of pre-processed CTD data, including low-pass w_{CTD}, as well as diagnostic plots. For details, see Section 2 below.

2. *Calculate vertical ocean velocity w_{ocean} with the LADCP_w_ocean utility.* Input: 1) 6 Hz time series of pre-processed CTD data. 2) RDI data file (PD0 format). Output: Edited (quality-controlled) vertical velocities, diagnostic data, as well as diagnostic plots. For details, see Section 3 below.

3. *Post-process w_{ocean} with the LADCP_w_postproc utility.* This utility carries out arbitrary data editing (removing bad measurements) and creates vertically gridded profiles from the edited w_{ocean} data. Data from uplooker and downlooker ADCPs from dual-headed LADCP systems can be combined into a single profile. Input: One or two LADCP_w_ocean output files, and a file with data-editing parameters. Output: Fully processed w_{ocean} profile. For details, see Section 4.3 below.

For processing, every profile must be assigned a unique *profile id* (usually numerical), which is used to construct file names and to select profile-specific processing parameters. Often, it makes sense to use the CTD station number as the *profile id*. In addition to the *profile id,* every processed profile is additionally associated with a *run label*, which can be any character string. This allows multiple processing runs for a single profile.

1.4 Input/Output Data

ADCP Input Data. Binary data in the Teledyne/RDI PD0 format are accepted as input. Supported instrument types include NB150, BB150, WH150, WH300, WH600, WH1200, and the Explorer DVL.

CTD Input Data. Either binary or ASCII 24 Hz CNV time-series files from SBE911plus systems are accepted as input. Alternatively, the CTD data can be supplied in a simple ASCII CSV format (Appendix A). In case of SBE CNV files, the header must include the latitude of the station, and the file must contain pressure (`prDM`), *in situ* temperature (`t090c` and/or `t190c`) and conductivity (`c0S/m` or `c0mS/cm` and/or `c1S/m` or `c1mS/cm`) fields. If the CTD file contains a header field called `station`, the content of this field is taken as the default *profile id.*

Output Data. All output files use a whitespace-delimited ASCII file format called the ANTS format. The "#" character is used for comments and metadata header lines; the string `nan` is used to indicate missing values. ANTS files can easily be read by many software packages, possibly after manually removing the headers. The file layout (association of field names with data columns) is defined by the last header line beginning with `#ANTS#FIELDS#`. Header lines beginning with `#ANTS#PARAMS#` define meta-data parameters. The `Matlab` script `loadANTS.m`, which resides in the installation directory of the LADCP_w software, can be used to load ANTS files, including metadata, into Matlab.

Diagnostic plots. All plots produced by the processing software are in Postscript (ps) format with loose bounding boxes (standard GMT output).
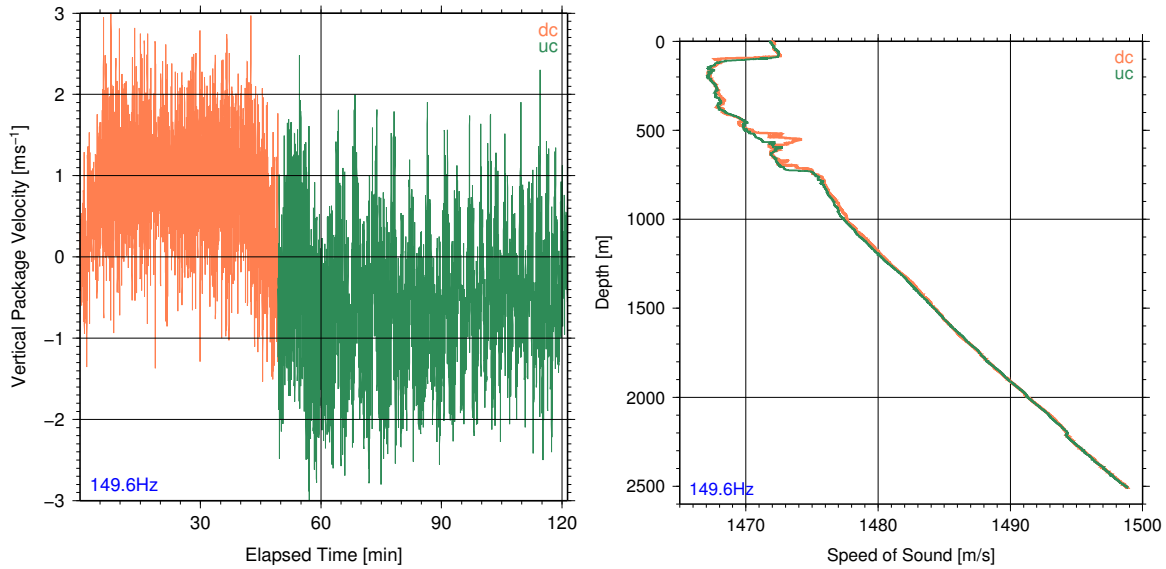
Figure 2: Example plots of output of `LADCP_w_CTD` from DIMES US2 station 149 in Drake Passage (Software V1.1). Left panel: Time series of vertical package velocity. Right panel: Sound speed profile.

2 Calculating Vertical Package Velocity (`LADCP_w_CTD`)

In a first processing step, 24 Hz CTD time-series data are pre-processed with the `LADCP_w_CTD` utility to derive cleaned 6 Hz time series of depth, sound speed, vertical package velocity, and temperature. The vertical package velocity is low-pass filtered to remove measurement noise; based on tests carried out with an early version of the processing software, a default low-frequency cut-off of 2 s is used.[2] Additionally, the minimum observed pressure is subtracted from all pressure measurements to ensure non-negativity.

`LADCP_w_CTD` takes the name of the CTD file as an argument and, often,[3] a profile id supplied with the `-i` command-line option. The preferred input formats of CTD files are SBE CNV binary and ASCII files (HEX CNV files are not supported at present). If CNV files are not available the CTD time series data can also be supplied in a simple ASCII CSV format (Appendix A). By default, `LADCP_w_CTD` only displays error messages. In order to see progress, use `-v 1`; for diagnostic output use `-v 2`. For example, the command

```
LADCP_w_CTD -i 8 -v 2 oc46802008.cnv
```

processes the data in the file `oc46802008.cnv` with diagnostic output on screen, and produces the following three output files:

`008.6Hz` Time-series of CTD measurements (pressure, temperature, conductivity), and derived quantities (depth, salinity, sound speed, vertical package velocity).

`008_wpkg.ps` Diagnostic plot of of vertical package velocity time series (e.g. Figure 2, left panel).

---

[2] The low-pass cutoff can be modified with a command-line option to `LADCP_w_CTD`.

[3] For CTD files with the correct profile id in the `station` header field, `-i` is not required.

185 008_sspd.ps Diagnostic plot of sound speed profile (e.g. Figure 2, right panel).

The user must ensure that the CTD time series used for vertical-velocity processing are free from significant glitches. Therefore, all diagnostic plots produced by LADCP_w_CTD should be inspected. (Figure 2 shows examples from a station occupied in Drake Passage on a fairly rough day for reference.) Pressure spikes, in particular, introduce package-velocity anomalies that typically cause the
190 time-lagging algorithm used to merge the CTD with the ADCP data (Section 3) to fail. Other errors in the CTD data often do not cause processing to fail, but they increase the vertical-velocity errors and the erroneous data should, therefore, be removed. Profiles for which the automatic data editing implemented in LADCP_w_CTD is insufficient must be pre-cleaned by replacing bad values in the input file with nan strings. *No scans must be removed from the CNV files that serve as input to*
195 *LADCP_w_CTD.*

Data transmission errors between the SBE 911plus underwater unit and the deck box cause CTD scans to be dropped, resulting in fewer than 24 CTD scans per second. As the SBE deck-box ignores this issue when time-stamping the data — it simply increases the elapsed time by $1/24$ s for each received scan — the SBE timestamps are not used for w_{ocean} processing. While the modulo-count
200 field in the SBE data can be used to determine where there are missing scans, I have not found a way to re-construct how many scans have been dropped from the recorded data. Therefore, profiles affected by significant transmission problems, e.g. due to dirty slip rings on a winch, can usually not be processed for vertical velocity. Profiles where the CTD data acquisition is restarted during the cast can usually also not be processed, either.

205 # 3 Calculating Vertical Ocean Velocity (LADCP_w_ocean)

3.1 Synopsis

In a second processing step the LADCP_w_ocean utility is used to calculate w_{ocean} from combined LADCP and CTD data. As input, LADCP_w_ocean requires a pre-processed CTD time series (Section 2) as well as a binary ADCP file. (The up- and downlooker data from dual-head LADCP systems
210 are processed separately, but the data can easily be combined during post-processing; Section 4.3.) LADCP_w_ocean requires one or two command-line arguments:

profile-id This argument is mandatory and usually numeric. It is used to select the CTD and ADCP input files, set profile-specific processing parameters, and to create output file names.

run-label This argument is optional and can be any string. It is used to distinguish different
215 processing runs for the same profile. For example, for dual-head LADCP systems the run labels DL and UL can be used for processing downlooker and uplooker data, respectively. If no run label is specified the label default is assumed. Each run label has its own associated output subdirectory, using the label as its name. The output directory must be created before processing.

220 It is not possible to specify input or output files for LADCP_w_ocean on the command line. Rather, profile-id and run-label are used to define the input and output filenames in the processing-configuration file (Section 3.2), which is also used to set the many configurable parameters controlling different aspects of processing. Some of the processing parameters can alternatively be set with command-line options, including the following:

225 **Screen verbosity (-v).** LADCP_w_ocean produces log output both on screen and in a log file. The -v option is used to set the verbosity level (0–3) for the screen output only, with -v 0 producing

7

only error messages, `-v 1` also including warnings (L0-2, with L2 being the most severe), `-v 2` producing a substantial amount of diagnostic output, and `-v 3` listing everything, including debugging messages. Default screen verbosity level is 1, and the log files always contain level 2 output.

Time lagging (`-i, -n, -w`). Accurate time lagging is crucially important for obtaining good vertical ocean velocities. The time-lagging algorithm involves three steps: i) An initial estimate is made based on the time when each profile reaches 10% of its maximum depth; this algorithm can be overridden by using the `-i` option. ii) A coarse-resolution time lag is calculated from 1 Hz CTD data. iii) A fine-resolution time lag is calculated using the full-resolution (6 Hz) CTD data. For steps ii and iii, the data are split into windows, controlled with the `-n` and `-w` options.

Setting water depth (`-h`). Knowledge of the water depth is important for editing measurements affected by previous-ping interference (PPI) and sidelobe contamination from the seabed. While the water depth is usually detected correctly by downlooking ADCPs, it has to be supplied manually for processing uplooker[4] data. The easiest way to do this is to specify the water depth with the `-h` command-line option to `LADCP_w_ocean`. Either a numerical value (water depth in meters) or the name of the corresponding downlooker w_{ocean} profile, which contains the water depth as meta data, can be provided as an option argument.

Setting vertical output resolution (`-o`). In contrast to horizontal LADCP velocities, w_{ocean} profiles from regions of weak acoustic backscatter can sometimes be improved by decreasing the vertical output resolution. Conversely, the output resolution can sometimes be increased in regions of strong backscatter to increase the vertical resolution. The default vertical resolution of 40 m should be appropriate for most data sets.

3.2 Processing Configuration File (`ProcessingParams`)

There are numerous parameters controlling many processing details. A complete list, including documentation, can be found in the file `defaults.pl` in the installation directory. The default parameter values are suitable for data sets collected with 300 kHz Workhorse instruments (WH300) with 8 m bin size; for different bin sizes and/or instruments some of the parameters likely need to be changed. The file `defaults.pl` should never be modified, however. Rather, non-default processing-parameter values should be set in a processing configuration file. The configuration file is read *after* processing the command-line options, i.e. definitions in the configuration file take precedence over command-line options.[5] There are several possible filenames for the configuration file. Given the run label DL, the following filenames are tried in order: `ProcessingParams.DL`, `ProcessingParams.default`, `ProcessingParams`. The first file that is found, is used. When `LADCP_w_ocean` is executed without a run label, only the latter two names are tried.

The processing configuration files are `perl` scripts. When they are executed, the current profile id and run label are stored in the variables `$PROF` and `$RUN`, respectively, allowing profile- and run-specific parameters to be selected with `if`-statements. While all processing parameters have suitable defaults, at the very least the LADCP and CTD input file names must be defined in the variables `$LADCP_file` and `$CTD_file`. The following example code assumes that the LADCP and CTD data for profile 13 can be found in the files `./LADCP/013DL000.000` and `./CTD/013.5Hz`, respectively:

---

[4]Even LADCP data from upward-looking instruments can be severely degraded by sidelobe contamination from the seabed!

[5]The only exception to this rule is that any expression supplied with the `-x` command-line option is executed after the configuration file has been processed.

```
$LADCP_file = sprintf("LADCP/%03dDL000.000",$PROF);
$CTD_file = sprintf("CTD/%03d.5Hz",$PROF);
```

If the CTD and/or LADCP input files use inconsistent numbering, a simple lookup table can be implemented, for example, as follows:

```
if (($PROF == 1) && ($RUN eq "DL")) {
    $LADCP_file = "LADCP/003DL000.000";
    $CTD_file   = "CTD/002.5Hz";
} elsif (($PROF == 2) && ($RUN eq "DL")) {
    $LADCP_file = "LADCP/002DL000.000";
    $CTD_file   = "CTD/003.5Hz";
} else {
    die("cannot determine input files for profile $PROF run $RUN");
}
```

noting that the perl operators `=` and `eq` check for numerical and lexical (string) equality, respectively. Of course, it is also possible to add profile-specific processing parameters to the same `if`-statement.

3.3   Processing Output Files

`LADCP_w_ocean` creates several output files, all in a subdirectory that uses the run label as its name. (If no run label is specified on the command line, the label `default` is used in the `ProcessingParams` file, but the output directory is called `profiles`.) If the output directory does not exist it is created. Assuming that the downlooker data from profile 13 have been processed successfully with the command

        LADCP_w_ocean 13 DL

the following data files are created:

DL/013.`log` Processing log output at verbosity level 2.

DL/013.`wprof` Gridded vertical velocity profiles from downcast; most fields are prefixed with `dc_`, `uc_` or `BT_`, indicating downcast, upcast and bottom-track data, respectively. For each depth bin, the following quantities are recorded: nominal depth (bin center), nominal height-above-bottom, mean depth and elapsed time of all contributing samples (`_depth` and `_elapsed`, respectively); bin-medians of 2-beam vertical velocities (`_w12` and `_w34`); bin-median of 3- or 4-beam vertical velocity (`_w`), mean-absolute-deviation from the 3-/4-beam median (`_w.mad`), as well as the number of samples per bin (`_w.nsamp`). (The 2-beam vertical velocities are primarily useful for diagnosing package-wake effects and bad beams.)

DL/013.`wsamp` Individual vertical velocity measurements (one record per bin for each ensemble). For each sample, the following information is recorded: ADCP ensemble number (`ensemble`), ADCP bin number (`bin`), elapsed time in seconds (`elapsed`), depth of measurement (`depth`), CTD depth (`CTD_depth`), downcast flag (`downcast`), 3-/4-beam vertical velocity (`w`), two separate 2-beam vertical velocities[6] (`w12` and `w34`), two quasi-horizontal horizontal velocity components (`u12` and `v34`), gridding residuals of the 3-/4- and 2-beam solutions (`residual`, `residual12`, `residual34`), vertical package velocity (`CTD_w`), acceleration (`CTD_w_t`) and its time derivative (`CTD_w_tt`), measured vertical velocity (`LADCP_w`), reference-layer vertical velocity (`LADCP_reflr_w`),

---

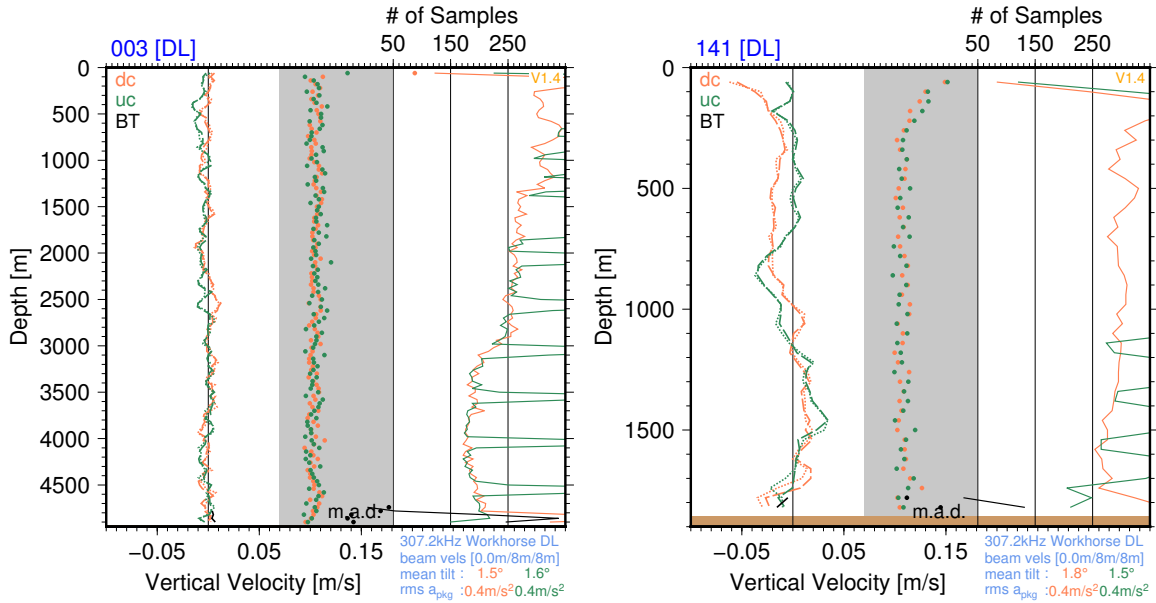[6]For coordinate transformations, see Appendix C.

Figure 3: Example `_wprof.ps` diagnostic plots from DIMES US2 cruise with weak (left panel) and strong (right panel) vertical velocities; software version is indicated in the upper-right corner of the figure panels; colors are used to distinguish between downcast (dc, green), upcast (uc, orange) and bottom-track (BT, black) data. Blue labels above the figure panels give `profile-id` and `run-label`. Summary information printed below the panel on the right includes instrument type and orientation, bin setup (blanking distance, pulse length and bin length), as well as *rms* tilt and vertical package acceleration observed during the cast. Each plot shows three types of data: i) 2-Beam vertical ocean velocity (median in each depth bin) plotted with dashed (w_{12}) and dotted (w_{34}) lines on the left and using the lower axis. ii) Corresponding mean-absolute-deviations (m.a.d.) plotted with bullets and also using the lower axis. iii) Corresponding number of samples plotted with solid lines on the right, using the upper axis.

estimate of the winch velocity (`winch_w`), error velocity (`errvel`), correlation (`correlation`), echo amplitude (`echo_amplitude`), volume scattering coefficient (`Sv`) calculated with the method of *Deines* (1999) with an additional empirical correction for remaining bin-dependent biases, package attitude (`pitch`, `roll`, `tilt` and `heading`), 3-beam flag (`3_beam`), and sound speed (`svel`).

`DL/013.tis` Time series of ADCP records (one record per ensemble) with merged CTD information: ensemble number (`ensemble`), elapsed time in seconds (`elapsed`), downcast flag (`downcast`), CTD depth (`depth`), sound speed at the transducer (`xducer_sound_speed`), package attitude (`pitch`, `gimbal_pitch`, `roll`, `tilt` and `heading`), vertical package velocity (`CTD_w`), time derivative of vertical package acceleration (`CTD_w_tt`), LADCP reference-layer vertical velocity (`LADCP_reflr_w` and `LADCP_reflr_w.sig`), and reference-layer ocean w (`reflr_ocean_w`).

In addition to those data files, a number of diagnostic plots are created. Figs. 3–9 show representative examples from high-quality profiles with both weak (left panels) and strong (right panels) vertical-velocity signals.
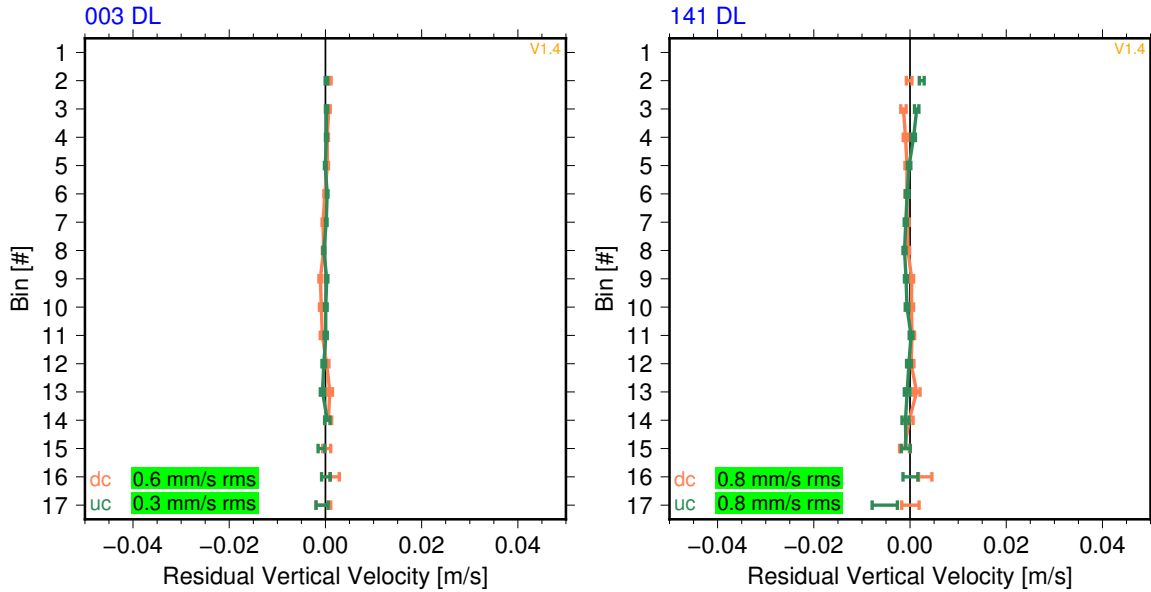
10

Figure 4: Example `_bin_residuals.ps` diagnostic plots for the two profiles of Figure 3. Each panel shows the mean residuals (with standard deviations) plotted against bin number (distance from ADCP transducer). The dc and uc labels printed inside the panel list downcast and upcast *rms* mean residuals in the block of bins with the best data (solid orange and green lines in the profiles); green, yellow and red background colors indicate data of progressively inferior quality.

DL/013_wprof.ps Downcast-, upcast- and bottom-tracked vertical velocity profiles, as well as gridding statistics (Figure 3). For data recorded in beam coordinates, the two 2-beam vertical velocities from both the up- and downcast are plotted separately with dashed and dotted lines, respectively. For data recorded in Earth coordinates, only a single solution is shown (e.g. upper right panel of Figure 16 in Appendix B). In addition to providing a summary of the data, this figure is useful for diagnosing package-wake effects and bad beams.

Below the figure panel on the right there is a legend with profile summary information, including instrument type and orientation, bin setup (blanking distance, pulse length and bin length), as well as *rms* tilt and vertical package acceleration observed during the cast. Large package tilts degrade the LADCP data; this problem can usually be mitigated by adding ballast to the CTD package and/or by lowering the winch speed during downcasts. Vertical package acceleration is dominated by heave due to surface waves moving the ship, i.e. it varies with sea state. (Vertical package acceleration ranges from $\approx 0.02\,\mathrm{m^2 \cdot s^{-1}}$ for profiles taken in flat calm conditions to $>0.6\,\mathrm{m^2 \cdot s^{-1}}$ for profiles collected in heavy seas.) There is evidence that the quality of LADCP data is affected by sea state. Abnormally large package tilts and accelerations are marked with yellow (moderately large) and red (very large) background colors; blue background indicates very little surface-wave related package motion, which may cause problems with time lagging.[7]

DL/013_bin_residuals.ps Mean residuals vs. distance from the ADCP transducer (bin number; Figure 4). Next to the profile summary plot, this is the most useful plot for diagnosing data problems. In particular, the residuals should be small and associated with little vertical struc-

---

[7]Profiles taken in close proximity to sea ice, for example, often require the `-l` command line option for processing.
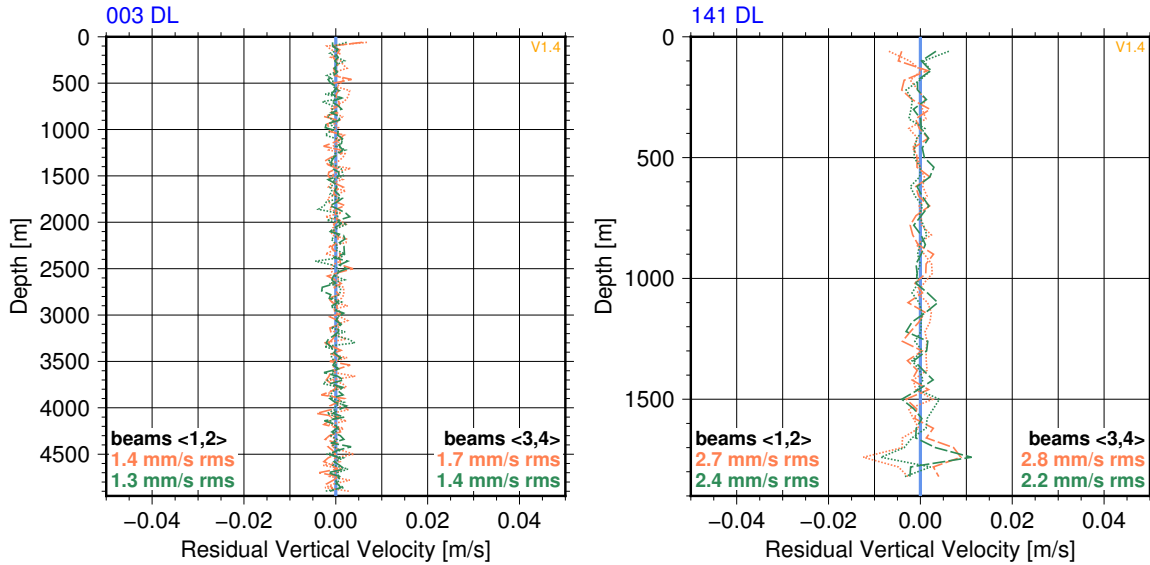
Figure 5: Example `_residual_profs.ps` diagnostic plots for the two profiles of Figure 3. Each panel shows profiles of mean beam-pair (dashed/dotted for beams <1,2>/<3,4>) and vertical-velocity residuals from the down- (orange) and upcasts (green). The overal *rms* values are printed inside the figure panels.

ture. For both down- and upcast *rms* values of the mean-residuals in a block of high-quality ADCP bins (indicated by the orange and green lines in the profiles) are printed inside the figure panels over a background of green, yellow or red, indicating progressively worse data quality. In profiles with large vertical velocities, comparatively larger residuals can be tolerated than in more quiescent regions.

DL/013_residual_profs.ps Profiles of vertical-velocity residuals from the two separate beam-pair estimates (Figure 5). This plot is useful for detecting anomalies affecting a particular part of the water column (e.g. due to biology near the surface, previous-ping interference, depth ranges with weak backscatter, ...) or a particular beam pair (e.g. due to package-wake effects). Anomalies indicating increased uncertainty near the seabed and the surface are commonly observed.

DL/013_wsamp.ps Time-depth plot of vertical ocean velocity (Figure 6). This plot is useful for diagnosing measurement artifacts, especially in comparatively shallow profiles.

DL/013_residuals.ps Time-depth plot of vertical velocity gridding residuals (Figure 7). This plot, too, is primarily useful for diagnosing measurement artifacts in shallow profiles.

DL/013_backscatter.ps Time-depth plot of acoustic volume-scattering coefficients (Figure 8). This plot is primarily useful for determining whether particular w signals could be biological artifacts (e.g. due to vertical plankton migration) or related to strong turbulence. After applying the correction of *Deines* (1999), the S_v values in each ADCP bin are corrected for remaining depth- and bin-dependent biases using *in situ* data. While this correction ensures horizontal banding in the _Sv plots, there remain apparently instrument-dependent biases of up to 5 dB, which must be removed manually before combining the acoustic backscatter data from upward- and

12
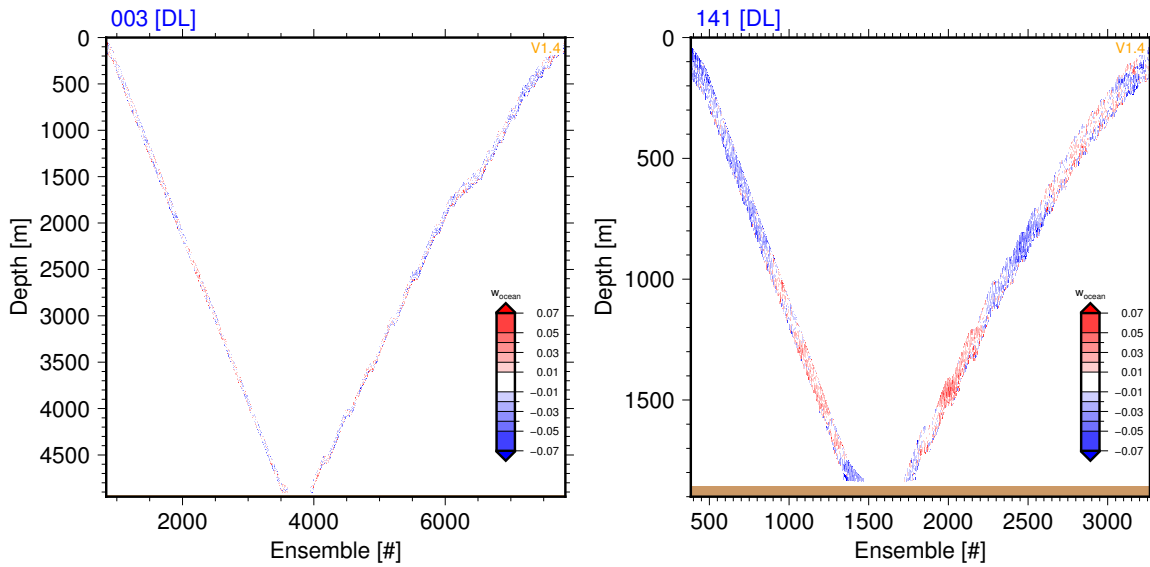
Figure 6: Example _wsamp.ps diagnostic plots for the two profiles of Figure 3. Each panel shows all ocean-velocity samples in time-depth space.
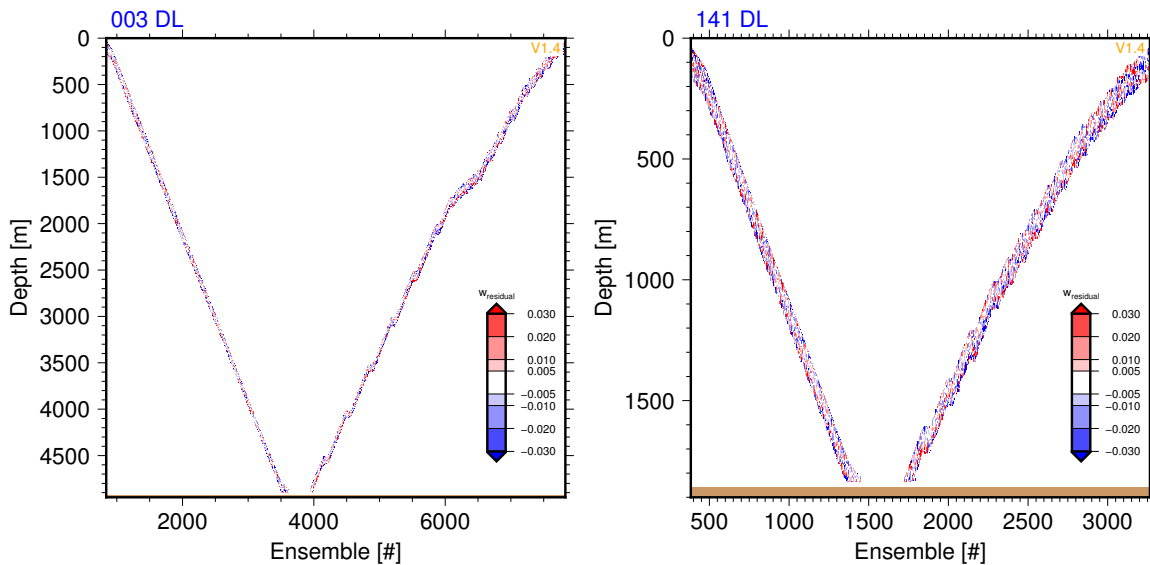
Figure 7: Example _residuals.ps diagnostic plots for the two profiles of Figure 3. Each panel shows all ocean-velocity residuals (differences between the individual measurements and the binned medians in the corresponding depth bins) in time-depth space.

downward-looking ADCPs. At present, calculation of S_v only works correctly for 300 kHz Workhorse ADCPs.

DL/013_time_lags.ps Time series of lag-correlation offsets used to merge the LADCP to the CTD
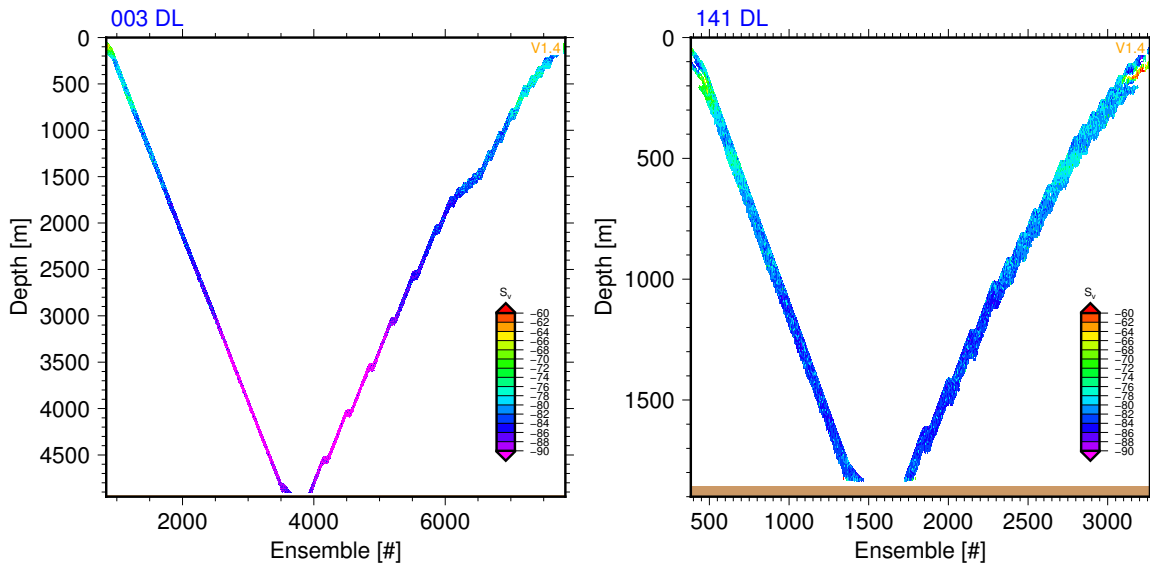
Figure 8: Example _backscatter.ps diagnostic plots for the two profiles of Figure 3. Each panel shows all acoustic volume scattering coefficients (S_v) in time-depth space.
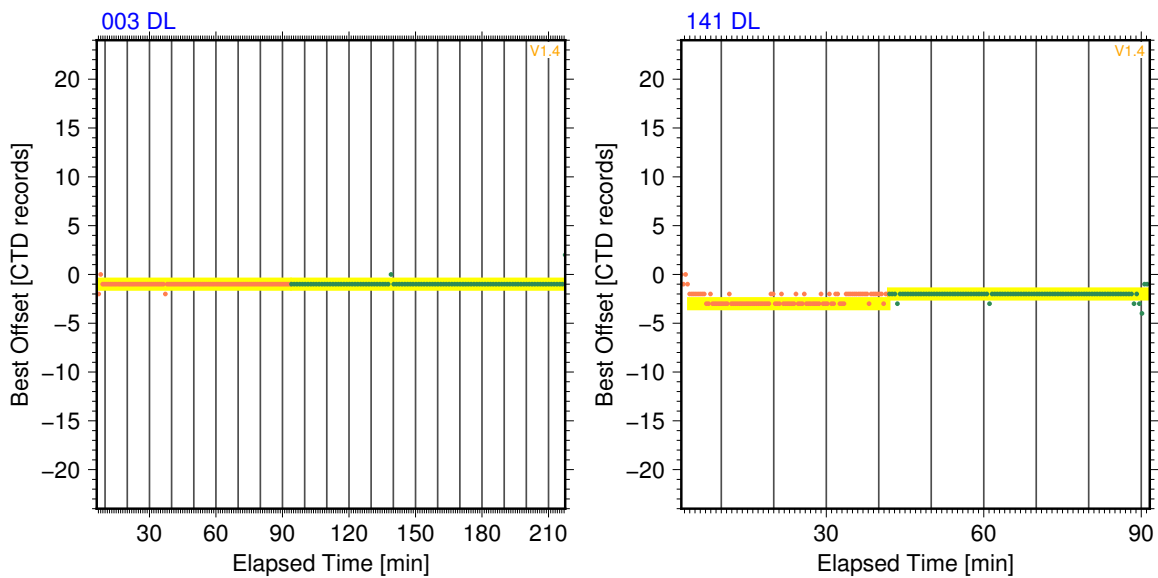
Figure 9: Example _time_lags.ps diagnostic plots for the two profiles of Figure 3. Each panel shows a time series of the lags required for optimal matching of the CTD to the ADCP data. Orange/green indicate downcast/upcast data; yellow bands underly periods that have passed time-lag filtering.

365   data (Figure 9). This plot is useful to verify that time-lagging was performing as intended and to diagnose dropped CTD scans (Appendix B.1).

3.4 Dealing With Processing Errors

Occasionally, data processing with `LADCP_w_ocean` fails with an error message. The most common problem is that the automatic time-lagging algorithm fails to determine the clock offset between the LADCP and CTD time series. Often, such time lagging problems can be corrected by manually determining an approximate time lag before processing as follows:

1. Process the data with zero time lagging (`-i 0 -u`) and with the "quick-and-dirty" (`-q`) option. This should always produce a `.tis` time-series output file, which is used in the next step.

2. Match the time series of `LADCP_reflr_w` to the time series of `CTD_w` by determining Δt so that `CTD_w` plotted against `elapsed` agrees with `LADCP_reflr_w` plotted against `elapsed+`Δt. Usually it is sufficient to estimate ΔT to within 10 seconds or so.

3. Re-process the data with `LADCP_w_ocean` using the `-i` command-line option or the variable `$initial_time_lag` in the processing configuration file to set the initial time-lagging guess to Δt.

4 Data Editing and Post-processing

4.1 Measurement Errors

Every processed w_{ocean} profile is contaminated by measurement errors that can include random noise, down-/upcast biases, winch-acceleration anomalies, as well as "glitches" caused by bad measurements that are not removed by the automatic data editing. While isolated bad measurements can be removed with the `LADCP_w_postproc` utility (Section 4.3) other errors, such as down-/upcast biases, are more difficult to deal with. As discussed below, the errors of vertical velocity profiles collected with dual-head systems can easily be quantified.

Apart from discrepancies between the two individual 2-beam solutions (which is is equivalent to large error velocities[8]) the most common indicator for problems with the vertical-velocity data are consistent differences (biases) between downcast and upcast profiles (Figure 10). Often, the upcast velocities are more biased than the downcast velocities. While, sometimes, the biases are approximately uniform throughout the water column (right figure panel), more often the biases are reduced during bottle stops (left panel), i.e. there can be significant vertical structure in the vertical-velocity errors of upcasts in particular. Depth-dependent errors are difficult to deal with in general. In case of the data set from the East Pacific Rise (example profile in left panel) vertical-wavenumber spectra of w_{ocean} indicate that vertical wavelengths shorter than $\approx$150 m in this data set are significantly degraded by measurement errors and should not be used *(Thurnherr et al.,* 2015). In case of the data set from the Gulf of Mexico (example profile in right panel), one might restrict the analysis to downcast profiles only or, alternatively, an empirically determined bias could be subtracted from each upcast profile. (Depth-independent biases do not affect calculation of finescale VKE.)

4.2 Combining Data from Dual-Head LADCP Systems (`LADCP_w_postproc`)

For w_{ocean} LADCP data collected with dual-head systems, measurement errors can easily be quantified as the UL and DL profiles are independent samples of the oceanic velocity field. Statistical independence results from the non-overlapping (in time) sampling of any depth layer by the two

---

[8]*Error velocity* is one of the diagnostic variables returned by RDI ADCPs. Error velocity is proportional to the difference between the two independent 2-beam measurements for w.
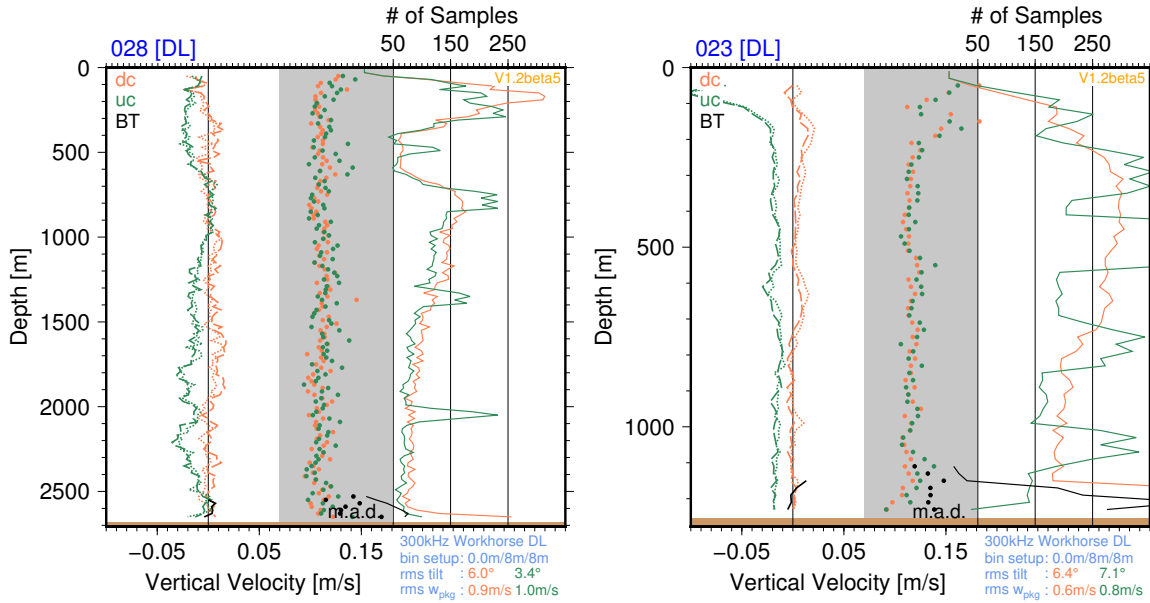
Figure 10: Example _wprof plots from two data sets associated with apparent downcast-/upcast vertical velocity biases. Left panel: East Pacific Rise crest; upcast velocities (green) are 1–3 cm·s⁻¹ too low, with reduced bias during long bottle stops. Right panel: Gulf of Mexico; upcast velocities are ≈2.5 cm·s⁻¹ too low throughout the profile.

instruments. With typical winch speeds of 50–60 meter per minute the two ADCPs sample the same depth layer $\approx$2–3 min apart, which is short compared to typical buoyancy periods and yet much longer than the time scales associated with surface-wave related vessel heave, which dominates the instantaneous w measurements almost everywhere.[9] As a result, correlation between DL and UL vertical-velocities is calculated as a simple quantitative indicator of profile quality when UL and DL data are combined with the `LADCP_w_postproc` utility. `LADCP_w_postproc` takes the DL and UL `.wsamp` files as input and creates a single profile and two diagnostic plots. For example, the command

```
LADCP_w_postproc DL/120.wsamp UL/120.wsamp
```

combines the measurements from `DL/120.wsamp` and `UL/120.wsamp` to create a combined w_{ocean} profile (`120.wprof`), as well as two diagnostic plots (`120_wprof.ps` Figure 11; `120_wcorr.ps`). The profile output from `LADCP_w_postproc` is similar to the the `.wprof` output from `LADCP_w_ocean`, except that there are no bottom-track and 2-beam solutions.[10] The diagnostic figure has the same layout as the _wprof diagnostic plots produced by `LADCP_w_ocean` (Figure 3); when two input files are used, the individual profiles are plotted with thin dashed and dotted lines, and the combined profile is plotted with heavy solid lines (right figure panel). In order to plot the BT solution as well, a downlooker profile can be supplied with the `-b` command-line option (`-b DL/120.wprof` in the example). The labels inside the figure panel show results from DL/UL correlation below a near-surface layer, indicated by the horizontal blue line. The most important diagnostic are the correlation

---

[9]In contrast to w, LADCP-derived horizontal velocities require data from the entire profile to constrain the flow at a particular depth.

[10]Vertical velocity profiles derived from combined DL/UL measurements should not be used to derive vertical kinetic energy and parameterized diffusivity estimates (Section 5.2).
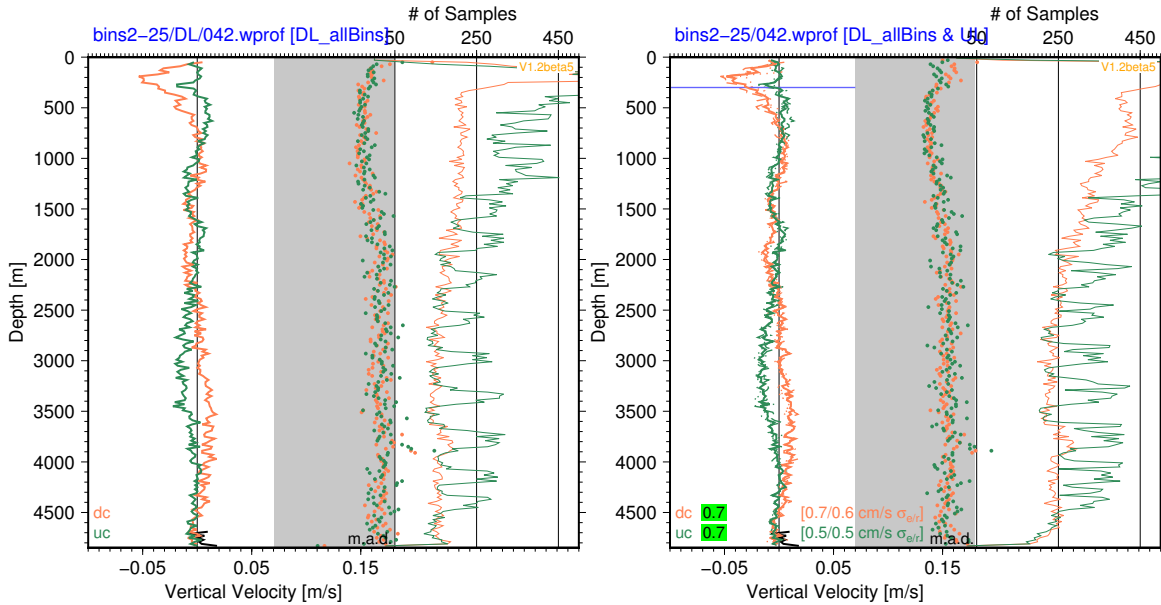
Figure 11: Example `_wprof.ps` diagnostic plots produced by `LADCP_w_postproc` showing a profile from the western tropical Pacific (2015 GO-SHIP P16N profile 120). Left panel: Using only the downlooker `.wsamp` input file. Right panel: Using both `.wsamp` input files (dual-head LADCP system); labels inside figure panel show results from DL/UL correlation below a near-surface layer (horizontal blue line); in addition to the correlation coefficients (on green, yellow or red backgrounds), the explained and residual standard deviations are given in square brackets.

coefficients, which are printed on green, yellow or red background, depending on the quality of the correlation. The explained and residual standard deviations are printed in square brackets to the right of the median profiles.

Figure 11 illustrates clearly how much harder it is to carry out QC with profiles derived from single instruments. Visually, there are no indications whether the apparent signals are real or measurement artifacts in the left panel, whereas the right panel clearly confirms the signals' reality. Consistent with this visual assessment, the DL/UL vertical velocities are highly correlated, in spite of the overall weakness of the signal. For vertical-velocity data collected with a single ADCP, where no UL/DL correlations can be calculated, an apparently universal k_z^{-2} power-law dependence of finescale vertical-wavenumber (k_z) VKE spectra *(Thurnherr et al.,* 2015) is useful, as it allows determination of both short-wavelength cutoff and instrument noise level at that wavelength (Section 5).

4.3 Manual Data Editing (`LADCP_w_postproc`)

In addition to combining the data from dual-head LADCP systems (Section 4.2) `LADCP_w_postproc` also provides a mechanism for manual editing of bad data. In many cases the bad data to be removed can be found quite easily by inspecting the diagnostic plots produced during data processing (Section 3.3). As additional help, some of the problems commonly encountered with automatically processed vertical velocity profiles are listed in appendices B.1–B.6.

Data editing instructions for `LADCP_w_postproc` are provided in a file called `./EditParams`, a

17

`perl` script that is executed for each of the `.wsamp` files. (Note that `./EditParams` is executed twice when combining the data from dual-headed LADCP systems into a single profile.) There is a small library of data-editing functions:

`output_resolution(40);` This statement sets vertical output resolution to 40 m, as appropriate for data collected in a region with weak acoustic backscatter. By default, the output resolution is taken from the input files (i.e. it is set by `LADCP_w_ocean`). Alternatively, it can be set with the `-o` command-line option to `LADCP_w_postproc`.

`bad_range_uc("depth",3700,"*");` Exclude the upcast vertical velocity data between 3700 m and the seabed from the gridded output profiles. The first argument can be any field name from the `.wprof` input file(s). Any number of "bad ranges" can be defined. The functions `bad_range_dc()` and `bad_range()` are also defined; the latter defines a common range for both downcast and upcast data.

In order to apply data editing only to specific profiles and/or run labels the editing functions must be made conditional with `if`-statements using the variables `$PROF` and `$RUN` as shown in the `ProcessingParams` example in Section 3.2. The following code example excludes the uplooker downcast data from processing of all profiles between 20 and 30:

```
if ($PROF>=20 && $PROF<=30 && $RUN eq "UL") {
    bad_range_dc("depth","*","*");
}
```

5 Calculating Finescale VKE and ϵ_{VKE} (`LADCP_VKE`

5.1 Preliminary Comments

Nearly everywhere instantaneous w_{ocean} is dominated by high-frequency (near-N) internal waves. As the typical magnitude of internal-wave related vertical velocities ranges from $\mathrm{mm\cdot s^{-1}}$ to $\mathrm{cm\cdot s^{-1}}$, LADCP data are particularly suitable in principle for estimating internal-wave VKE. To quantify total VKE, vertical-wavenumber (k_z) spectra derived from the w_{ocean} profiles must be integrated over the entire internal-wave wavenumber range. This is not usually possible, because the long-wavelength cutoff of the internal-wave range is not known. However, observations covering a wide range of environmental parameters (latitude, density stratification, Turner angle, water depth, . . .) and dynamical regimes (equatorial thermocline, Drake Passage, Luzon Strait, open abyssal ocean, . . .) show that finescale VKE density $\propto k_z^{-2}$, and that the VKE density level is $\propto \epsilon$ *(Thurnherr et al.,* 2015). The software described here carries out all the manual data editing described in the paper automatically, producing results that are consistent not only with the original microstructure data sets but with another one that were not used in the original analysis (Figure 1).

The k_z^{-2} dependence of the VKE spectra implies that total VKE is dominated by large vertical scales, emphasizing the problem of not knowing the large-wavelength cutoff required for spectral integration. However, the universality of the VKE vertical-wavenumber power law allows well constrained estimates of VKE density in the internal wave band by fitting the power law to observed spectra and sampling the fitted function at an arbitrary wave number. In *Thurnherr et al.* (2015) the VKE power levels are quantified by p_0 [in units of $\mathrm{m^2\cdot s^{-2}\cdot(rad/m)^{-1}}$], the intercept of the power-law fit carried out in log-space, i.e. p_0 is the VKE density at wavenumber $1\,\mathrm{rad\cdot m^{-1}}$, corresponding to a vertical wavelength of 6.3 m. This short wavelength can cause confusion because it is not within the finescale range. While this fact does not matter, the confusion can easily be avoided by sampling VKE density at a different wavenumber. For example, $p_{\mathrm{fs}} = p[k_z = 0.1\mathrm{rad}m^{-1}] = 100 \times p_0$ may be more palatable

for plotting than p_0 as it represents VKE density at wavelengths of ≈ 65 m, well within the expected internal-wave range.

5.2 Calculating p_0 and ϵ_{VKE} with LADCP_VKE

In order to calculate p_0 and apply the VKE finestructure parameterization for turbulent dissipation (ϵ_{VKE}) the utility LADCP_VKE is used. As input, it takes one or more .wprof files, created either with LADCP_w_ocean (Section 3) or with LADCP_w_postproc (Section 4.3). *When both DL and UL data are available, the two single-head .wprof files should be fed to LADCP_VKE, rather than combining the data from the two instruments with LADCP_w_postproc (Section 4.2) and feeding the resulting .wprof file to LADCP_VKE.* By default LADCP_VKE produces a .VKE data file, as well as a diagnostic plot (_VKE.ps; Figure 12). LADCP_VKE splits each profile into *windows* for calculating the spectra. For each spectral window, the output data files produced by LADCP_VKE contain the following fields:

widx Index of spectral window, counting downward from 1 near the surface; an additional bottom window (see below) has widx = -1.

depth, depth.min, depth.max Center depth in meters, as well as upper and lower limits of the spectral window.

hab Center height above the seabed (in meters) of the spectral window.

nspec Number of w_{ocean} profiles used to determine each spectrum. E.g. nspec = 4 when spectra are calculated from dual-headed ADCP data using both down- and upcast data and there are no long gaps in any of the profiles.

w.nsamp.avg For each input file the median number of w_{ocean} samples in the input data used to calculate the spectra is calculated. (The median is used to avoid biasing the estimates by bottle stops.) w.nsamp.avg is then set to the average of these medians.

pwrdens.0, pwrdens.1, ... VKE power spectral densities, averaged from all input files, in units of $\mathrm{m}^2 \cdot \mathrm{s}^{-2} \cdot (\mathrm{rad/m})^{-1}$; the corresponding vertical wavenumbers (wspec::k.0, wspec::k.1, ... in units of $\mathrm{rad} \cdot \mathrm{m}^{-1}$) and wavelengths (wspec::lambda.0, wspec::lambda.1, ... in units of meters) are included in the file metadata.

pwr.tot, pwr.fs VKE power integrated across the entire spectrum and across the finescale wavenumber range, respectively. Note that these powers are not corrected, e.g. for removal of the means.

p0 VKE power density of a k_z^{-2} (fixed-slope) power-law fit sampled at $k_z = 1 \, \mathrm{rad} \cdot \mathrm{m}^{-1}$.

p0fit.rms, p0fit.r, p0fit.slope, p0fit.slope.sig Statistics for assessing how well the observed spectra conform to a k_z^{-2} power-law: p0fit.rms is *rms* discrepancy between observed VKE and the best-fit k_z^{-2} power-law; p0fit.r is the correlation coefficient (in log-log space) of finescale VKE density vs. vertical wavenumber; p0fit.slope and p0fit.slope.sig give the best-fit power-law slope to the data.

eps.VKE VKE-finescale-parameterization estimate of kinetic energy dissipation in units of $\mathrm{W} \cdot \mathrm{kg}^{-1}$, calculated only when all of the following conditions are met:

1. Profile is poleward of $3°$ of latitude. This cutoff is little more than a guess based on inspection of plots from the 2015 US GO-SHIP P16N cruise.

19

2. k_z^{-2}-fit in log-log space has *rms* misfit `p0fit.rms <= 0.4` (as in *Thurnherr et al.,* 2015, where this cutoff yielded the best overall agreement between VKE and microstructure).

3. Power-law slope derived from linear fit in log-log space is approximately -2 (`p0fit.slope` between -3 and -1; this range of slopes corresponds approximately to `p0fit.rms <= 0.4`).

4. Spectral power and wavenumber are significantly correlated (`p0fit.r <= -0.4`). This cutoff corresponds approximately to `p0fit.rms <= 0.4`.

5. VKE spectral levels are significant $[(p_0/c)^2 \geq 5 \times 10^{-11}\,\mathrm{W \cdot kg^{-1}}$, where c is the empirical parameterization constant relating p_0 to $\sqrt{\epsilon}$ (see below)]. The limiting value was chosen primarily based on DIMES data as the minimum value that is is necessary to filter out the low-p_0 outliers apparent at low values of dissipation in Fig. 2 of *Thurnherr et al.* (2015). The limiting value necessarily has to be smaller than the "working limit" of the method ($\approx 2 \times 10^{-10}\,\mathrm{W \cdot kg^{-1}}$; Section 5.3 below) to allow for scatter in the p_0 estimates.

   Since only samples with small turbulence levels are affected by this cutoff, averages are not sensitive its value. In regions of low turbulence levels there will be few spectral samples passing this cutoff test, however. Where there are sufficient samples available it appears that this cutoff does not bias suitable averages even in regions of weak turbulence. For example, an average ϵ_{VKE} profile derived from the DIMES US2 data from the open South Pacific ocean, where turbulence levels are considered "oceanic background," is consistent with the corresponding mean microstructure profile (Section 5.3 below).

The additional checks (3–5), which were not used in the analysis of Thurnherr et al. (2015), primarily remove estimates with low ϵ_{VKE}. These erroneous low-ϵ estimates biased both curve fits used to determine empirical scaling constant c in the original analysis identically, resulting in a uniform (independent of turbulence level) 30% high-bias of the parameterization. The same bias is observed with the additional data set not included in the original analysis (DIMES UK2). In order to correct for this bias, the scaling constant was increased by 20% to $0.026\,\mathrm{s}^{-\frac{1}{2}}$, resulting in unbiased estimates (Figure 1).

By default, the VKE spectra are calculated in half-overlapping windows neither exceeding 32 samples nor 600 m vertical wavelength. (For profiles binned at the default 40 m resolution, 320 m-wide windows are used by default.) Data from a 150 m-deep near-surface layer are ignored by default, i.e. the center depth of the top window is typically at 310 m. In order to avoid bottom gaps, an additional window is created near the seabed unless the `-b` command-line option is used — note that this bottom window overlaps more than 50% with the window above. By default, the spectra are calculated from combined downcast/upcast data but there `-d` and `-u` can be used to use downcast or upcast data alone. The `-d` and `-u` options affect all input files. Before calculating the spectra, means are removed (changeable with the `-o` option), and the spectra are corrected for attenuation of the high wavenumbers due to depth-averaging by the instrument and during processing *(Polzin et al.,* 2002; *Thurnherr,* 2012).

Similar to LADCP-derived horizontal velocities *(Polzin et al.,* 2002), the effective vertical resolution of LADCP-derived w_{ocean} is much coarser than the bin length used to acquire the data. Deviations in VKE spectra from the apparently universal k_z^{-2} power law *(Thurnherr et al.,* 2015) allow visual determination of the noise-cutoff wavelength from spectral plots. By default, `LADCP_VKE` uses a 100 m vertical-wavelength cutoff which is suitable for many typical LADCP data sets. The short-wavelength cutoff can be modified with the `-c` command-line option.

`LADCP_VKE` produces diagnostic plots that show both VKE spectra and derived ϵ_{VKE} profiles (Figure 12). Gaps in VKE profiles (e.g. left figure panel) are common. In general, the number of gaps tends to increase with decreasing VKE levels. High-quality profiles have fewer gaps than profiles associated with measurement problems. The overlapping windows allows a simple visual assessment

Figure 12: Example _VKE.ps diagnostic plots from DIMES US2 cruise with weak (left panel) and strong (right panel) vertical velocities (same profiles as used in Figure 3). Samples from each window are plotted in blue, with darker shades indicating deeper depths. Main panels: p_0-normalized VKE spectral density vs. vertical wavenumber; individual window spectra are plotted in blue, with dots indicating spectra that do not pass the tests required for estimating ϵ_{VKE} (Section 5.2); solid and dotted pink lines show mean spectra calculated from only the good and from all window spectra, respectively; the finescale ranges used for the spectral fits are marked with the heavy line of the mean spectra (100–320 m in these cases); the mean finescale spectra should lie entirely on top of the green-shaded areas, which encompass factor-2 uncertainties in the derived ϵ_{VKE} estimates. Insets: ϵ_{VKE} profiles derived from the spectra that pass the quality checks.

of the profile consistency. In case of the example profiles shown in Figure 12, the scatter of the ϵ_{VKE} estimates suggest that the turbulence levels below 2500 m are not very tightly constrained.

570   A better assessment is possible when independent estimates ϵ_{VKE} are compared. For data collected with dual-headed LADCP systems, separate estimates can be derived from the DL and UL profiles. For single-instrument LADCP profiles, separate estimates can be calculated from the downcast and upcast data. In case of the left example profiles shown in Figure 12, separate downcast/upcast profiles indicate that the apparent near-surface intensification of turbulence is likely real (not shown).

575   5.3   Comparison With Microstructure

Based on comparisons with simultaneous microstructure data, there is an approximately universal relationship between LADCP-derived VKE levels and ϵ down to turbulence levels of $\approx 2 \times 10^{-10}$ W·kg^{-1} (Fig. 2 in *Thurnherr et al.* (2015)). As a result, many of the individual profiles of simultaneous fine- and microstructure derived ϵ from regions of strong turbulence resemble each other qualitatively

580   (Figure 13). In order to obtain quantitative agreement within factor 2, averaging can be used; the Drake-Passage averages of VKE- and microstructure-derived ϵ from 8 joint profiles shown in the left panel of Figure 14 agree better than within factor two, and much better than within the boostrapping-derived uncertainties. While the corresponding estimates from Gregg-Henyey-Polzin
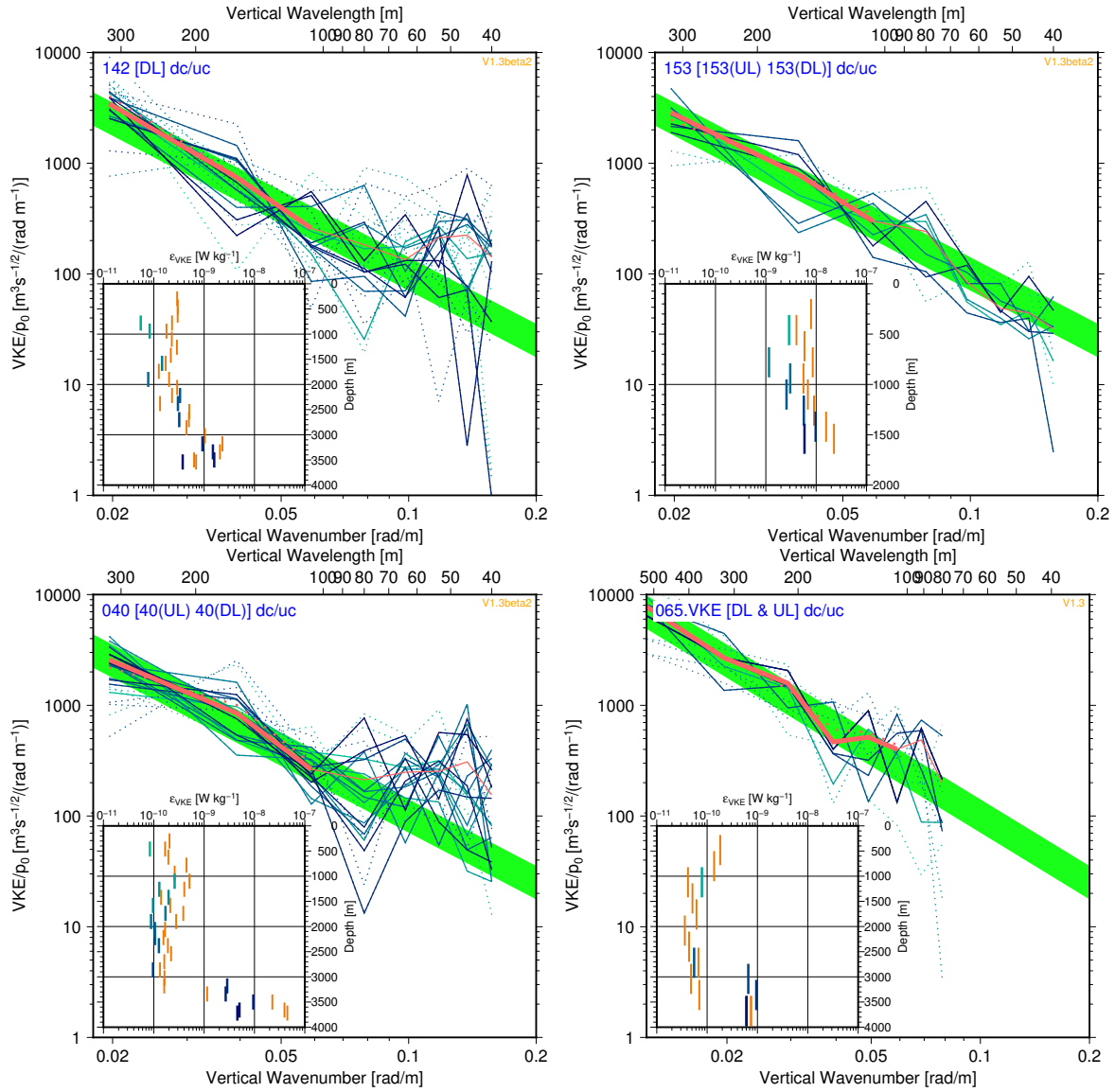
21

Figure 13: VKE diagnostic plots from profiles with strong turbulence (c.f. Figure 12); in addition to the VKE-derived estimates, each inset shows a corresponding profile from simultaneous microstructure in orange. Clockwise from top left: DIMES US2 profile from Drake passage, IWISE profile from Luzon Strait, DoMORE-2 profile from MAR-flank canyon, and DIMES UK2 profile from Drake Passage.

scaling (shear-strain method) also agree with the mean microstructure values within the bootstrapping uncertainties, the agreement is much less close than that of the VKE estimates.

At turbulence levels below $\approx 2 \times 10^{-10}\,\mathrm{W \cdot kg^{-1}}$ the relationship between VKE and ϵ no longer remains the same and the VKE parameterization method is biased low. This is the reason why LADCP_VKE does not produce ϵ_{VKE} estimates for spectra with low-p_0 values (Section 5.2). The VKE-
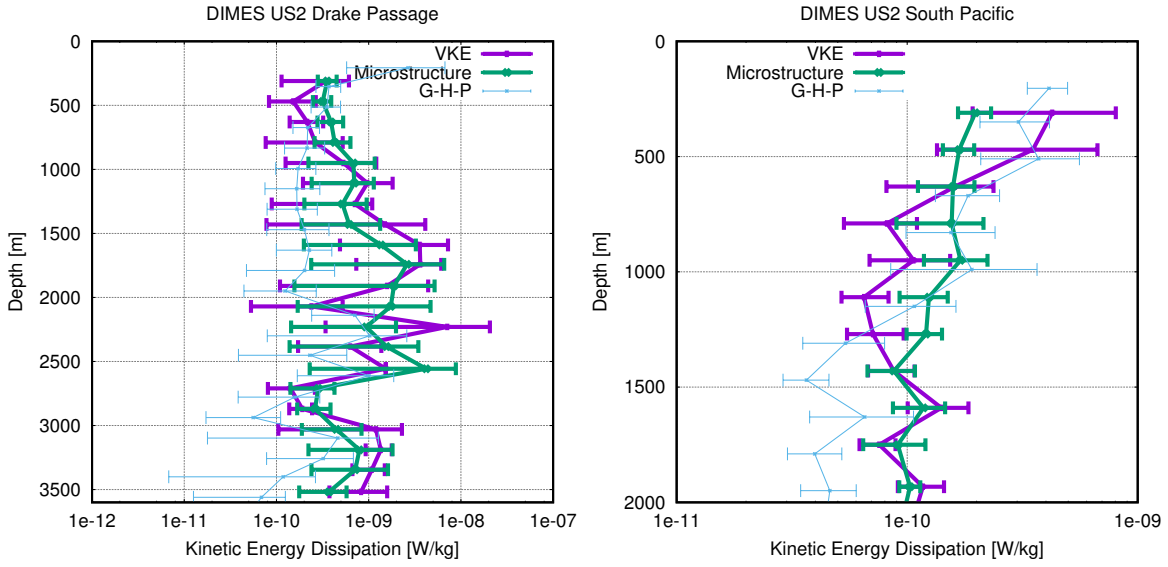
Figure 14: Mean profiles of fine- and microstructure-derived kinetic energy dissipation with 95% confidence intervals from boostrapping; the average from the *Kunze et al.* (2006) implementation of the shear-strain method (Gregg-Henyey-Polzin scaling) is shown for comparison with the VKE method. Left panel: DIMES US2 8-profile average from Drake Passage. Right panel: DIMES US2 93-profile average from the open South Pacific.
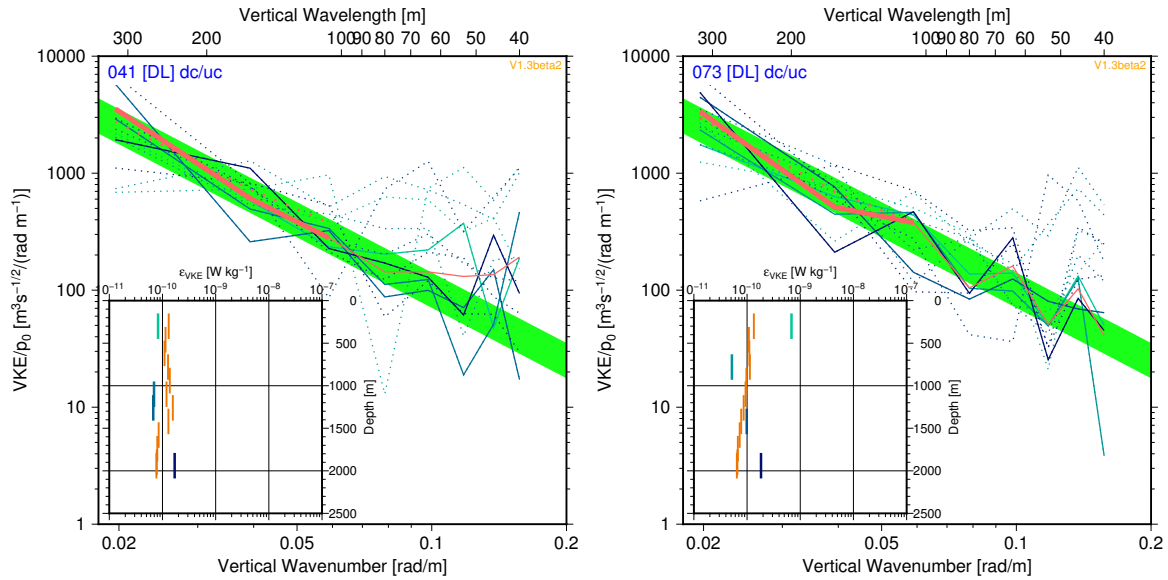

Figure 15: VKE diagnostic plots from two example profiles with weak turbulence (c.f. Figure 13), both from DIMES US2.

derived estimates from individual profiles in such regions of weak turbulence contain many missing

values and where there are values these are often not very consistent with simultaneous microstructure data (Figure 15). There is clear evidence (not shown) that the relationship between ϵ and VKE density at weak turbulence levels depends on the density stratification, indicating that the present parameterization should be improved. Nevertheless, even in regions of weak turbulence, sufficiently averaged profiles of ϵ_{VKE} have been found to be consistent with simultaneous microstructure profiles within factor 2 (Figure 14, right panel, noting that the factor 2 has not been included in the errorbars). Even such highly averaged profiles are clearly unsuitable for many purposes, however, including, for example, inferences of buoyancy flux convergence or divergence from $\partial\epsilon_{\mathrm{VKE}}/\partial z$. As in the case of the mean Drake Passage profile, the mean VKE-derived profile agrees better with microstructure than the corresponding profile derived with the shear-strain method as implemented by *Kunze et al.* (2006).

A   Alternative CSV File Format For CTD Data

The preferred formats for CTD time-series data are binary or ASCII SBE CNV files, because they contain useful meta-data. The simple ASCII CSV (comma-separated values) format described here allows for fewer consistency checks and, therefore, requires additional care. The following assumptions are made for CSV ASCII CTD time series files:

1. 24 Hz sampling frequency

2. pressure in units of dbar

3. temperature in units of °C using ITS-90

4. conductivity in units of mS·cm^{-1}

Each CSV ASCII CTD file has a single header line listing the latitude, longitude and, optionally, the number of the profile, followed by the data records with scan number, pressure, *in situ* temperature and conductivity. Scan numbers must be consecutive and start at 1. Missing values are allowed, but comments and empty lines are not. The following shows the beginning of an example CSV ASCII CTD file with station number (7) and two missing values:

```
-53.939,86.57,7
1,12.525,3.8788,31.499201
2,12.433,3.8789,
3,12.468,3.8788,31.499325
4,12.419,,31.499388
5,12.489,3.8788,31.499013
6,12.419,3.8788,31.499075
```

B   Common Data Problems

Most of the plots in this appendix were produced with older versions of the processing software and some look somewhat different from plots produced with the current software version. The software version used to produce the plots is indicated in the top right corners of the figure panels.
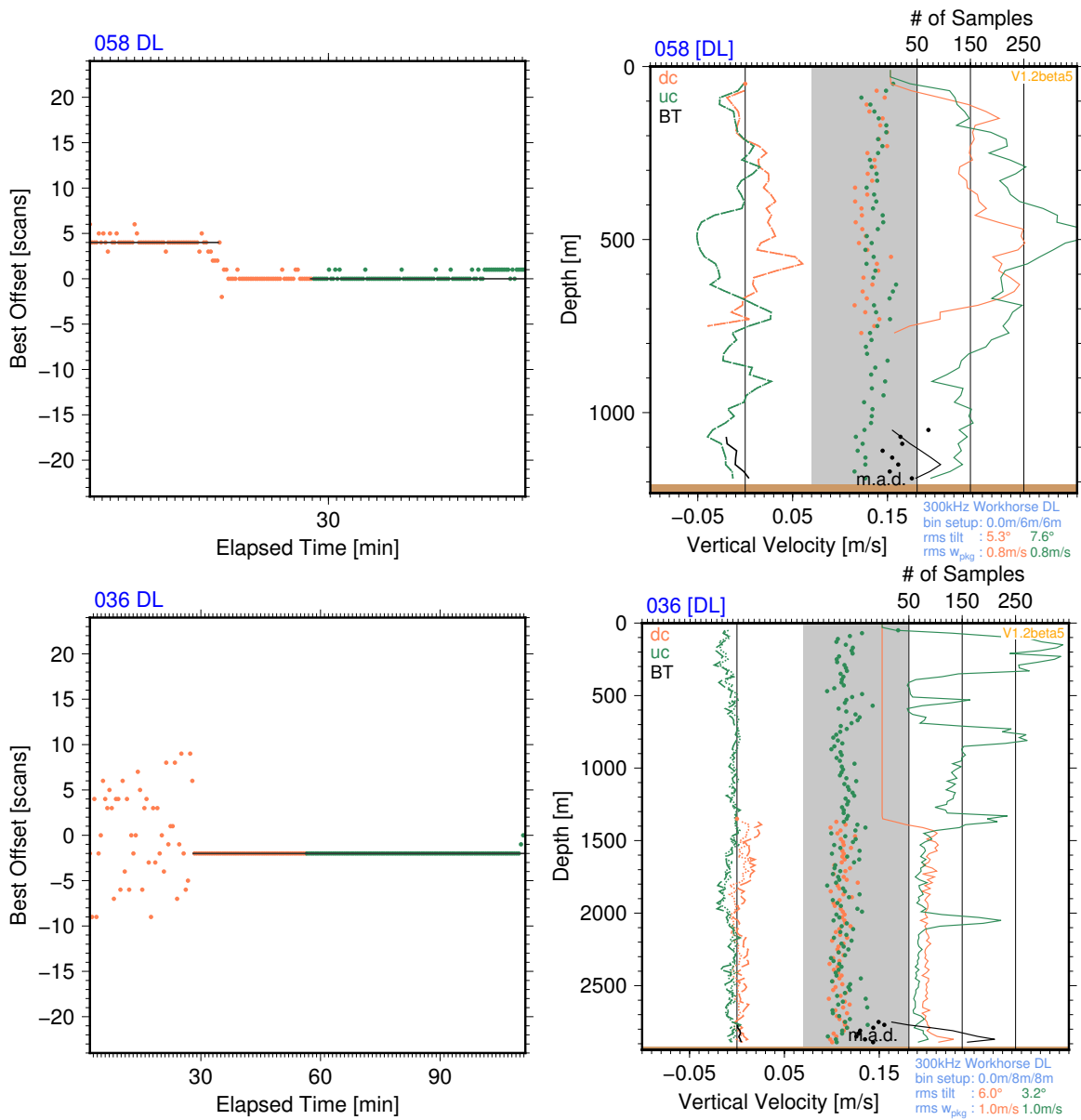
Figure 16: Diagnostic plots from two example profiles (upper and lower panels, respectively) with dropped CTD scans. Left panels: _time_lags plots. Right panels: _wprof plots.

B.1 Dropped CTD Scans

As described in Section 2 data transmission problems in the CTD system cause dropped scans. As long as only one or two "scan-drop events" occur during a profile this problem is usually easily detectable in the _time_lags plots (Figure 16). Profiles with more than two "scan-drop events," on the other hand, usually cannot be processed with LADCP_w_ocean at all. In the example shown

25

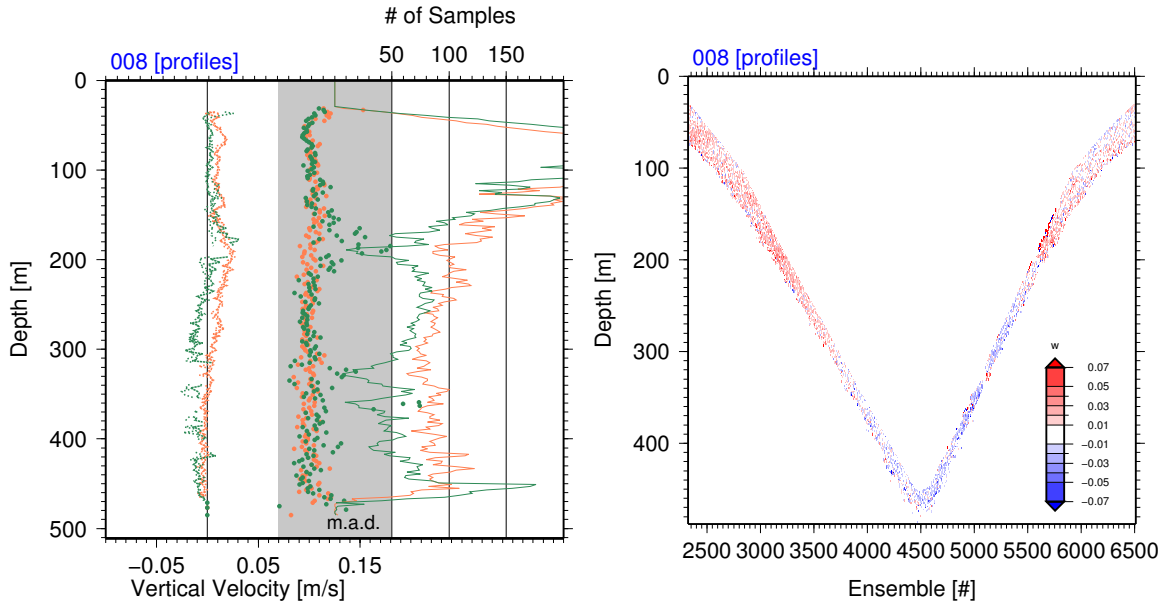Figure 17: Diagnostic plots from a profile from the equatorial Pacific with insufficient sampling; software V1.1. Left panel: _wprof plot. Right panel: _wsamp plot.

in the upper two figure panels three CTD scans (1/8 s worth of data) were dropped approximately 15 min after the beginning of the cast. As the pre-drop time lag is used for the downcast (solid line) the downcast data after the dropped scans are bad and are removed by the automatic editing. [Alternatively, the -p option of LADCP_w_ocean can be used to carry out "piece-wise" time lagging. By default, LADCP_w_ocean lags the downcast and upcast data separately.] In the example shown in the bottom two panels of the figure, the number of scans dropped was too great for the time-lagging algorithm to work correctly at the beginning of the cast.

B.2   Insufficient Sampling & Profile Gaps

Bad ADCP data, e.g. due to insufficient acoustic scattering or large instrument tilts, can cause insufficient sampling and, in extreme cases, gaps in the vertical-velocity profiles. While such data gaps are not problematic *per se* (Section 1), there are often vertical-velocity artifacts where the number of samples per depth bin is low, including at the edges of profile gaps, as well as near the sea surface and seabed. In the example shown in Figure 17, there are insufficient (<40, in this case) upcast samples in the following depth ranges: 186–196 m, 316–338 m, 356–368 m, 402–414 m, in addition to couple of isolated single-record gaps. At the edges of some of these gaps (e.g. just above 185 m in Figure 17, and also at both edges of the wake-affected upcast data gap shown in the right panel of Figure 18), there are clear artifacts that must be removed during post-processing. Alternatively, the gaps in this profile can be avoided altogether by processing (or post-processing) at a coarser vertical resolution.

B.3   Package-Wake Effects

It is a fairly common observation in LADCP work that uplooker downcast data and/or downlooker upcast data are affected by package wakes. In the context of vertical-velocity processing, these
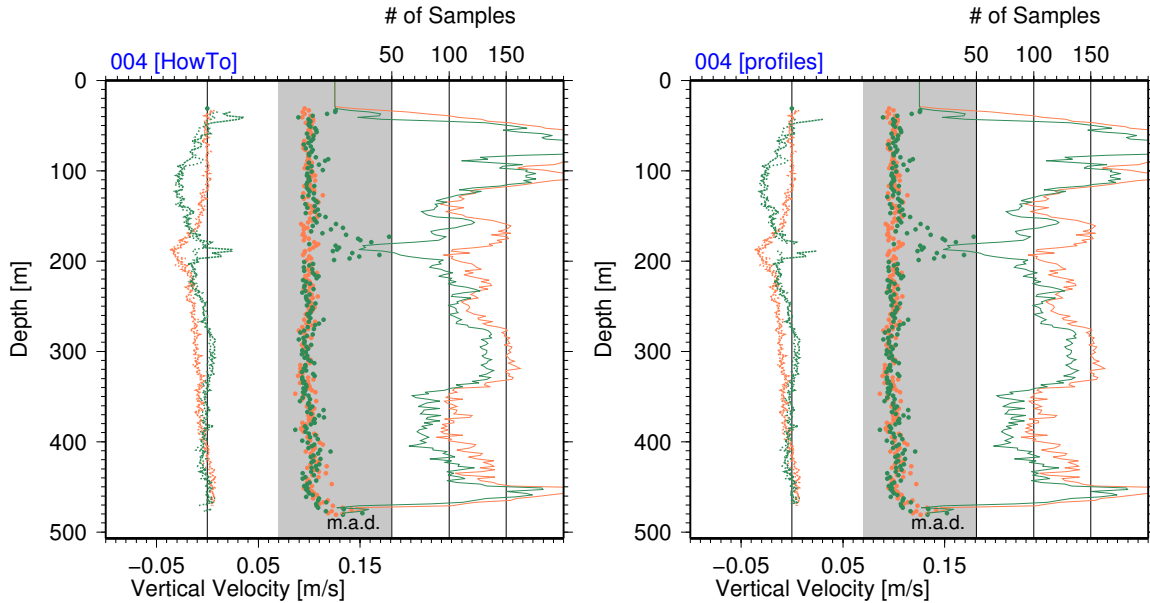
Figure 18: Diagnostic _wprof plots from an equatorial Pacific profile affected by package wake; software V1.1. Left panel: Profile processed with the requirement of $\geq$20 samples per depth bin. Right panel: Profile processed with the requirement of $\geq$40 samples per depth bin.

wakes manifest themselves as vertically coherent layers where the two independent 2-beam solutions for w_{ocean} disagree significantly. In the example shown in Figure 18 package-wake effects affect the upcast data between 50 and 100 m and, more importantly, the wake causes an erroneous apparent
655 upwelling peak centered at 190 m in one of the two 2-beam upcast solutions, which must be removed during post-processing.

It is important to note that the difference between the two 2-beam solutions is identical (except for a scaling constant) to the so-called ADCP *error velocity.* Since error velocity is used as a data-editing criterion in LADCP_w_ocean, the most severely wake-affected samples are discarded automatically
660 during processing, leading to gaps in the w_{ocean} profiles and gap-edge artifacts (Section B.2), which can be difficult to attribute to wake effects (right panel in Figure 18).

B.4   Moving Organisms

Not all vertical motion measured by ADCPs near the sea surface is due to vertically moving water, as at least some of the organisms giving rise to the acoustic backscatter required for ADCP measure-
665 ments are capable of rapid vertical movement. There are regions where vertical plankton migrations dominate upper-ocean ADCP vertical-velocity measurements at certain times of the day (e.g. *Fischer and Visbeck,* 1993b). In the example shown in Figure 19 there is a likely $\approx$10 m-thick layer of upward-moving plankton rising from 160 to 60 m during the cast (left panel). While this vertically moving layer does not appear to affect the processed w_{ocean} profiles significantly (right figure panel) there
670 are apparent downcast artifacts associated with another thin acoustic scattering layer near 160 m.

Vertical velocities in the upper ocean should generally be treated with particular caution, especially in regions of high biological productivity. In a data set collected in the northeastern Gulf of Mexico, for example, consistently strong apparently downward motion was observed in the upper
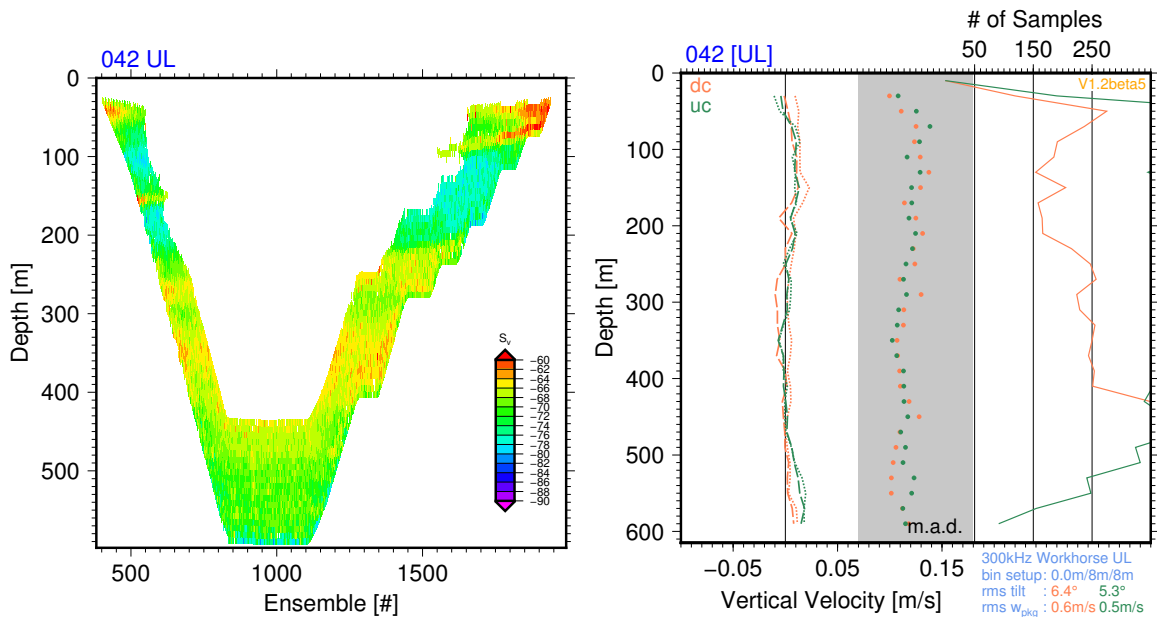
Figure 19: Diagnostic plots from a profile with a likely ≈10 m-thick layer of vertically moving plankton rising from 160 to 60 m during the cast; software V1.0. Left panel: _Sv plot; the anomalous vertical structure of acoustic backscatter below 400 m is due to imperfections in the backscatter calculation algorithm. Right panel: _wprof plot.
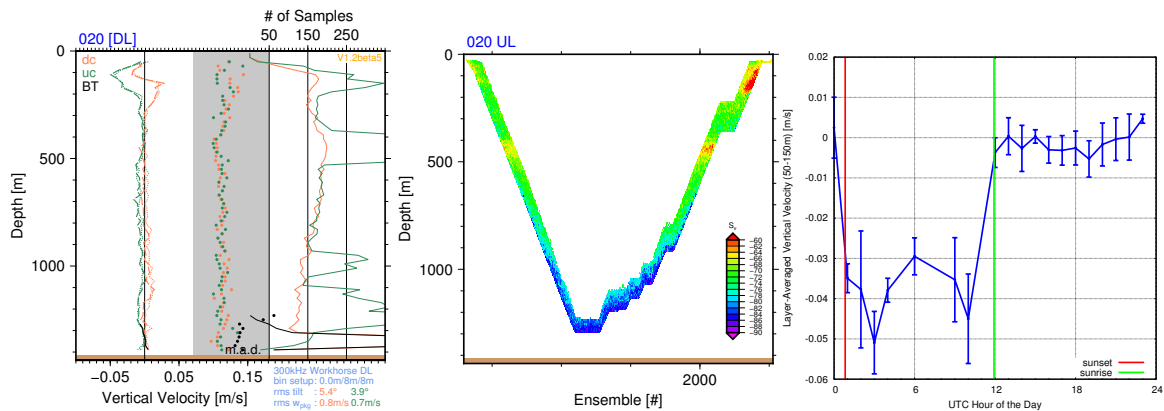

Figure 20: Upper-ocean vertical velocity signals in the northeastern Gulf of Mexico likely caused by biology. Left and middle panels: Diagnostic _wprof and _backscatter plots from an example profile with strong apparent downwelling observed during the upcast in the upper 200 m of the water column. Right panel: Average w_{ocean} between 50 and 150 m vs. hour of the day for all profiles from this site.

200 m in the profiles taken between sunset and sunrise, but not during daylight hours (Figure 20). While inconsistent with diel vertical plankton migration, the observed downward motion is associated with strong acoustic backscatter anomalies (middle panel), consistent with the hypothesis that the
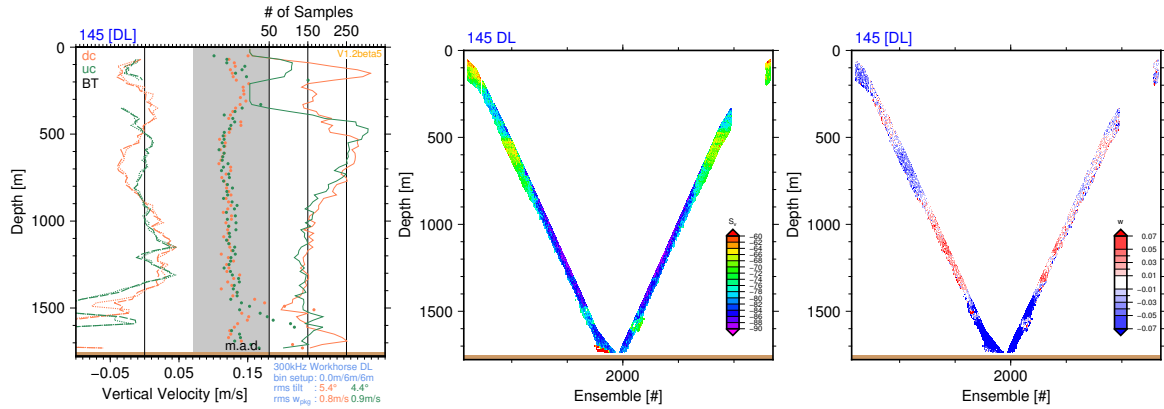
675

28

Figure 21: Diagnostic plots from a profile in a region with very strong turbulence. From left to right: _wprof, _Sv and _w plots, respectively.

apparent motion is caused by swimming organisms. The consistent apparently downward motion can be explained by radially outward swimming organisms: Since vertical velocities are calculated as averages of the along-beam velocities from two opposing beams (Appendix C), radial outward motion results in a false apparent downward velocity. This error is due to the violation of the assumption of horizontal homogeneity of the velocity field that underlies ADCP velocity measurements.

B.5 Boundary Effects

In addition to biology, there are other causes for potential contamination near the sea surface, including reduced sampling, interference from acoustic instruments mounted on the surface vessel, sidelobe reflections from its hull and the sea surface, as well as high-frequency vertical motion associated with (long) surface-gravity waves. Near the seabed, reduced sampling and sidelobe reflections from steep topography can adversely affect the data. (When pinging simultaneously, sidelobe contamination from the seabed affects uplooker as well as downlooker data, which makes it important that the water depth is set correctly when processing uplooker profiles; Section 3.1.)

B.6 Strong Turbulence

High levels of turbulence in regions such as Drake Passage and Luzon Strait can affect LADCP-derived vertical-velocity profiles. The example profile shown in Figure 21 was collected slightly east of the crest of a meridionally trending ridge blocking deep flow through Luzon Strait. At the time of observation, there was strong eastward bottom-intensified flow at the location. Following the sloping topography, the eastward flow is associated with strong downwelling (left figure panel). Both the elevated acoustic backscatter between 1500 and 1600 m (center panel) and the bursts of upward motion embedded within the strongly downwelling background (right panel) are consistent with the signatures of large turbulent eddies in this layer of extreme vertical shear of the zonal flow ($\approx 0.5\,\text{m}\cdot\text{s}^{-1}$ over 100 m). The vertical velocities associated with the turbulent eddies contaminate both downcast and upcast profiles of w_{ocean} (left panel).

29

C Velocity Transformations

C.1 Beam-Coordinate ADCP Data

The following algorithm is used to derive vertical velocities from LADCP data acquired in radial beam coordinates:

1. Using linear interpolation, the along-beam velocities are re-sampled at the levels of the nominal bin centers

$$z_{\mathrm{bin}} = z_{\mathrm{ADCP}} + \Delta_{\mathrm{bin}} \cos \tau, \tag{1}$$

where Δ_{bin} is the center-line (along the ADCP yaw axis) distance between the ADCP transducer and the bin center, and

$$\tau = \cos^{-1}(\cos \phi \cos \rho) \tag{2}$$

is the instrument tilt (deviation from the vertical), with ϕ and ρ denoting pitch and roll angles as measured by a set of gimbals aligned with beampairs <1,2> (ϕ) and <4,3> (ρ), respectively. TRDI ADCPs do not measure ϕ but, rather, ϕ_{RDI}, from which ϕ can be derived as follows *(RD Instruments,* 1998)

$$\phi = \tan^{-1}(\tan \phi_{\mathrm{RDI}} \cos \rho). \tag{3}$$

2. The beam velocities (b_1, b_2, b_3, b_4) are transformed into the instrument coordinate system used by TRDI ADCPs *(RD Instruments,* 1998): v'_{12}, v'_{43}, w'_{avg}, and e_{RDI}, where v'_{12} and v'_{43} are the quasi-horizontal[11] velocity components in the roll and pitch planes, respectively, i.e.

$$v'_{12} = \frac{b_1 - b_2}{2 \sin \beta} \tag{4}$$

$$v'_{43} = \frac{b_4 - b_3}{2 \sin \beta}, \tag{5}$$

with β denoting the transducer beam angle from the vertical, $w'_{\mathrm{avg}} = (w'_{12} + w'_{34})/2$, with w'_{12} and w'_{34} denoting the two independent two-beam measurements of quasi-vertical velocity, i.e.

$$w'_{12} = \frac{b_1 + b_2}{2 \cos \beta} \tag{6}$$

$$w'_{34} = \frac{b_3 + b_4}{2 \cos \beta}, \tag{7}$$

and

$$e_{\mathrm{RDI}} = \frac{b_1 + b_2 - b_3 - b_4}{2\sqrt{2} \sin \beta} \tag{8}$$

$$= \sqrt{2} \tan \beta (w'_{12} - w'_{34}) \tag{9}$$

is the TRDI "error velocity", which is scaled by ≈ 0.5 ($\sqrt{2} \tan \beta \approx 0.51$, for $\beta = 20°$) for convenient comparison with the horizontal velocity components *(RD Instruments,* 1998).

3. The quasi-vertical velocities in instrument coordinates[12] (w'_{12}, w'_{34} and w'_{avg}) are rotated into a coordinate system where the vertical velocities are aligned with the gravitational vector,[13] using

---

[11]Ignoring instrument tilt.

[12]This does *not* include e_{RDI}, which is always reported in instrument coordinates.

[13]This system is sometimes called "horizontal coordinates" *(RD Instruments,* 1998). It differs from earth coordinates in that the horizontal velocities are not corrected for heading.

the rotation matrix (A1) from *Lohrmann et al.* (1990) for data collected with downward-looking instruments (for which $w > 0$ implies upward velocity).[14] Specifically,

$$w = w' \cos \phi_c \cos \rho - v'_{12} \cos \phi_c \sin \rho + v'_{43} \sin \phi_c \tag{10}$$

with

$$\phi_c = \sin^{-1} \frac{\sin \phi \cos \rho}{\sqrt{1 - \sin^2 \phi \sin^2 \rho}}. \tag{11}$$

Note that while transformation expression (10) looks superficially identical to the one used by TRDI ADCPs *(RD Instruments,* 1998),

$$w = w' \cos \phi \cos \rho - v'_{12} \cos \phi \sin \rho + v'_{43} \sin \phi, \tag{12}$$

it is different in that the rotation angle in the pitch plane ϕ_c is more accurate than ϕ used in the TRDI instrument-to-earth transformation, with the errors increasing with increasing instrument roll.

C.2 Earth-Coordinate ADCP Data

For LADCP data acquired in earth coordinates, the transformation from beam to horizontal coordinates is carried out by the instrument firmware. In instrument coordinates,

$$w'_{12} = w'_{\text{avg}} + \frac{1}{2}(w'_{12} - w'_{34}) \tag{13}$$

$$w'_{34} = w'_{\text{avg}} - \frac{1}{2}(w'_{12} - w'_{34}). \tag{14}$$

Combining with (9) yields

$$w'_{12} = w'_{\text{avg}} + \frac{e_{\text{RDI}}}{2\sqrt{2} \tan \beta} \tag{15}$$

$$w'_{34} = w'_{\text{avg}} - \frac{e_{\text{RDI}}}{2\sqrt{2} \tan \beta}, \tag{16}$$

where β is the transducer beam angle from the vertical as before. In order to derive beampair vertical velocities from earth-coordinate ADCP data,

1. earth coordinate vertical velocities are rotated into instrument coordinates ($w_{\text{avg}} \to w'_{\text{avg}}$),

2. expressions (15) and (16) are used to calculate w'_{12} and w'_{34}, and

3. the resulting beampair instrument velocities are rotated into a horizontal coordinate system.

The velocity transformations carried out by TRDI ADCPs are not as accurate as those derived with the algorithm described in Section C.1 for two reasons, both related to large tilt angles: i) Properly configured TRDI ADCPs use bin remapping at large tilt angles *(RD Instruments,* 1998). This nearest-neighbor interpolation scheme is less accurate than linear interpolation (e.g. *Ott,* 2002). ii) The instrument-to-earth transformation expression (12) is an approximation valid for small tilt angles *(Lohrmann et al.,* 1990). No evidence has been found so far suggesting that the inaccuracies associated with expression (12) are significant. Therefore, no attempt has been made to implement a correction.

---

[14]For upward-looking instruments, the first and third columns of the transformation matrix A1 are negated (first and second r.h.s. terms in expression (10)), which is equivalent to adding $180°$ to the roll angle *(RD Instruments,* 1998).

References

Deines, K. L., 1999: *Proceeding, CWTMC'99 (IEEE)*.

Firing, E. and R. Gordon, 1990: Deep ocean acoustic Doppler current profiling. *IEEE Fourth Working Conf. on Current Measurements*, 192–201.

Fischer, J. and M. Visbeck, 1993a: Deep velocity profiling with self-contained ADCPs. *J. Atm. Oc. Tech.* **10**, 764–773.

Fischer, J. and M. Visbeck, 1993b: Seasonal variation of the daily zooplankton migration in the Greenland Sea. *Deep Sea Res. I* **40**, 1547–1557.

Kunze, E., E. Firing, J. M. Hummon, T. K. Chereskin, and A. M. Thurnherr, 2006: Global abyssal mixing inferred from Lowered ADCP shear and CTD strain profiles. *J. Phys. Oceanogr.* **36**, 1553–1576.

Lohrmann, A., B. Hackett, and L. P. Røed, 1990: High resolution measurements of turbulence, velocity and stress using a pulse-to-pulse coherent sonar. *J. Atm. Oc. Tech.* **7**, 19–37.

Ott, M. W., 2002: An improvement in the calculation of adcp velocities. *J. Atm. Oc. Tech.* **19**, 1738–1741.

Polzin, K., E. Kunze, J. Hummon, and E. Firing, 2002: The finescale response of lowered ADCP velocity profiles. *J. Atm. Oc. Tech.* **19**, 205–224.

RD Instruments, 1998: ADCP coordinate transformation: Formulas and calculations. *RDI Manual*.

Thurnherr, A. M., 2010: A practical assessment of uncertainties in full-depth velocity profiles obtained with Teledyne/RDI Workhorse Acoustic Doppler Current Profilers. *J. Atm. Oc. Tech.* **27**, 1215–1227.

Thurnherr, A. M., 2011, March): Vertical velocity from LADCP data. *Proceeding, CWTMC'11 (IEEE)*.

Thurnherr, A. M., 2012: The finescale response of lowered ADCP velocity measurements processed with different methods. *J. Atm. Oc. Tech.* **29**, 597–600.

Thurnherr, A. M., S. S. Jacobs, P. Dutrieux, and C. F. Giulivi, 2014: Export and circulation of ice cavity water in Pine Island Bay, West Antarctica. *J. Geophys. Res.* **119**, 1754–1764.

Thurnherr, A. M., E. Kunze, J. M. Toole, L. St. Laurent, K. J. Richards, and A. Ruiz-Angulo, 2015: Vertical kinetic energy and turbulent dissipation in the ocean. *Geophys. Res. Lett.* **42**, 7639–7647.

Visbeck, M., 2002: Deep velocity profiling using Lowered Acoustic Doppler Current Profilers: Bottom track and inverse solutions. *J. Atm. Oc. Tech.* **19**, 794–807.